



Norwegian University of  
Science and Technology

# Application of Virtual Synchronous Machines for Integration of Offshore Wind Turbines into the Power System of Offshore Oil and Gas Platforms

**Eivind Risan Mathisen**

Master of Energy and Environmental Engineering

Submission date: June 2016

Supervisor: Elisabetta Tedeschi, ELKRAFT

Co-supervisor: Jon Are Suul, ELKRAFT

Norwegian University of Science and Technology  
Department of Electric Power Engineering

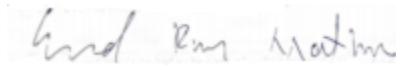


## Preface

This is a master thesis in Electrical Energy Engineering at the study program Energy and Environmental Engineering at NTNU. The thesis was carried out during the spring semester of 2016, and was developed in collaboration with SINTEF Energy Research.

It is assumed that the reader of this document has a background in electric power engineering and has a principal understanding of power systems and control theory.

Trondheim, 06-2016

A handwritten signature in black ink, reading "Eivind Risan Mathisen". The signature is written in a cursive style and is centered on the page.

Eivind Risan Mathisen

## Acknowledgment

I would like to thank my supervisors Elisabetta Tedeschi and Jon Are Suul for their great help and guidance through several meetings and email correspondence.

I also want to thank my family for their continuous support during my education and during the writing of this thesis.

E.R.M.

## Summary

This thesis addresses the technology known as "Virtual Synchronous Machines" and studies an application where it is used to integrate offshore wind turbines into the power systems of oil and gas platforms. The virtual synchronous machine is a technology which involves the controlling of an electric power converter in order to mimic the properties of a traditional synchronous machine. This thesis studies a fictional system where the virtual synchronous machine control strategy is applied to a converter that connects a battery bank to the power system of an offshore platform. A wind turbine is also connected to the same platform and this thesis looks at the interactions between the battery bank, the wind turbine, and the rest of the power system of the platform.

A model of this system has been constructed and implemented into a simulation program. A lot of work went into experimenting and exploring the capabilities of this model. This process enabled the identification of several relevant test cases to simulate and present.

This thesis presents the results of several test cases that involve events such as rapid increase in electrical load and variations in the wind power from the turbine. The focus is on the control strategies of the various components, how they interact with each other and how they effect the power grid of the platform.

The simulations show that a battery bank that is controlled by a virtual synchronous machine is able run in parallel with a traditional synchronous generator and a wind turbine and they demonstrate how these components distribute the electrical load between themselves. The simulations also demonstrate how the battery bank and a wind turbine are able operate in island mode where the controls of the battery bank is controlling the frequency of the electrical grid. These controls also respond to changes in load, which means the gas turbine can be turned of when there is enough wind power available. Overall these simulations indicate that this implementation has a practical suitability when it comes to the connection of offshore wind power to oil and gas platforms.

## Summary in Norwegian

Denne masteroppgaven omhandler teknologien som heter ”virtuelle synkronmaskiner” og ser på muligheten for å bruke denne teknologien for å koble offshore vindkraft sammen med kraftsystemene til olje- og gassplattformer. Den virtuelle synkronmaskinen er et konsept som går ut på å kontrollere en kraftomformer på en slik måte at den vil etterligne egenskapene til en tradisjonell synkronmaskin. Denne masteroppgaven studerer et fiksjonelt system hvor denne kontrollstrategien blir brukt til å kontrollere kraftelektronikken til en batteribank som er koblet til kraftsystemet til en olje og gassplattform. Denne plattformen har også en vindturbin koblet til kraftsystemet sitt og denne masteroppgaven skal se på samspillet mellom batteribank, vindturbin og kraftsystemet til plattformen.

En modell av dette kraftsystemet har blitt konstruert og implementert inn i et simuleringsprogram. Mye arbeid gikk med på eksperimentering og utforsking av egenskapene til denne modellen. Dette arbeidet gjorde det mulig å identifisere en rekke test scenarioer som var relevante for videre simulering og analyse.

Resultatene fra simuleringen av disse test scenarioene har blitt presentert i denne masteroppgaven. Scenarioene inneholder hendelser slik som rask endring i elektrisk last og variasjoner i vindkraft. Fokuset har ligget på kontrollstrategiene til de ulike komponentene samt hvordan disse har påvirket hverandre og kraftsystemet til plattformen.

Simuleringene viser at batteribanken som blir driftet som en virtuell synkronmaskin kan operere i parallell med tradisjonelle synkrongeneratorer og vind turbiner og demonstrerer hvordan disse komponentene fordeler den elektriske lasten mellom hverandre. Simuleringene viser også at vindturbinen og batteribanken klarer å operere i øy-modus, hvor frekvensen til det elektriske nettet på plattformen blir bestemt av kontrolleren til batteribanken. Denne kontrolleren responderer også til endringer i last slik at gassturbinen på plattformen kan slås av under gode vindforhold. Alt i alt er disse simuleringsresultatene en indikasjon på at denne implementasjonen av en virtuell synkronmaskin er praktisk anvendbar for tilkobling av offshore vindkraft til olje og gassplattformer.

## Task Description

### Application of Virtual Synchronous Machines for integration of offshore wind turbines into the power system of offshore oil and gas platforms

*The emissions and operating costs of offshore oil and gas platforms can be significantly reduced by electrification and power supply from the onshore power system. Another alternative to reduce the CO<sub>2</sub> and NO<sub>x</sub> emissions is the integration of offshore wind power into their isolated power systems. This can make it possible to turn off gas turbines on the platform in periods with good wind conditions. If local battery energy storage is also introduced, gas turbines can also be turned off in periods with light or varying loads. However, in case no synchronous machines are in operation, the ac frequency, voltage and power balance in the on-board power system must be controlled by the power converters interfacing the wind turbines and/or the energy storage. As a result, the local power system will be an isolated grid dominated by power electronic converters and without any physical, rotating inertia. Therefore, the control system for the converters should be designed for being able to operate in a converter-dominated scenario as well as in parallel with traditional synchronous generators. The concept of Virtual Synchronous Machines (VSM) can be a suitable control approach for fulfilling these requirements, since it allows for emulating the main characteristics of inertia and damping inherent to synchronous machines. Thus, VSMs are expected to ensure simple integration and parallel connection of VSCs in systems with existing generators.*

*The focus of the Thesis will be on the study of VSM applicability for interfacing wind turbines with offshore oil and gas platforms. At least one possible implementation scheme for VSM control should be simulated for this purpose, and the performance and practical suitability for the target application should be analyzed under both steady-state and contingency conditions. The performance in comparison or in combination with other possible control strategies for power electronic converters can be also discussed and analyzed.*

## Acronyms

**SRF** Synchronous reference frame

**VSM** Virtual synchronous machine

**VSC** Voltage source converter

**PWM** Pulse-width modulation

**PLL** Phase locked loop

**PV** Photovoltaics

**SG** Synchronous generator

**IGBT** Insulated-gate bipolar transistor

**DFIG** Doubly-fed induction generator

**PMSG** Permanent magnet synchronous generator

**JIP** Joint industry project

**PCC** Point of common coupling

**IOR** Improved oil recovery



# List of Figures

2.1	Turbine and Generator [21]	11
2.2	House diagram for load sharing [20]	12
2.3	CO <sub>2</sub> emissions from platforms on the norwegian continental shelf [19]	13
2.4	Block diagram of a synchronous machine and turbine	14
2.5	Inner control loop	19
2.6	Outer control loop	19
3.1	One line diagram of the system	24
3.2	VSM topology	26
3.3	Droop-based reactive power controller [10]	28
3.4	Simplification of wind turbine	31
3.5	Control of wind turbine VSC	32
4.1	Test case 1.1: Active power a)	37
4.2	Test case 1.1: Active power b)	37
4.3	Test case 1.1: Various system speeds	39
4.4	Test case 1.1 without VSM: Various system speeds	40
4.5	Test case 1.2: Active power a)	41
4.6	Test case 1.2: Active power b)	41
4.7	Test case 1.2: Various system speeds	42
4.8	Test case 2.1: Active power	44
4.9	Test case 2.1: Speed	44

4.10	Test case 2.2: Reactive power . . . . .	46
4.11	Test case 2.2: Load voltage magnitude . . . . .	46
4.12	Test case 3.1: speed . . . . .	48
4.13	Test case 3.2: speed and power . . . . .	49
A.1	Maturity of wind turbine technology . . . . .	55
B.1	SG parameters . . . . .	56
B.2	System overview . . . . .	57
B.3	Wind turbine VSC in Simulink® . . . . .	58
B.4	Gas turbine and SG . . . . .	59

# List of Tables

- 3.1 Parameter values of the VSM . . . . . 28
- 3.2 Impedance values of the electric load . . . . . 33
- 3.3 Grid impedance values . . . . . 34
  
- 4.1 Test case 1.1: Parameter values . . . . . 36



# Contents

Preface . . . . .	i
Acknowledgment . . . . .	ii
Summary . . . . .	iii
Summary in Norwegian . . . . .	iv
Task Description . . . . .	v
Acronyms . . . . .	vi
List of figures . . . . .	vii
List of tables . . . . .	ix
<b>1 Introduction</b>	<b>1</b>
1.1 Motivation . . . . .	1
1.2 Objectives . . . . .	3
1.3 Scope of Work . . . . .	4
1.4 Limitations . . . . .	4
1.5 Approach . . . . .	6
1.6 Structure of the Report . . . . .	7
<b>2 Background</b>	<b>9</b>
2.1 Traditional Offshore Oil and Gas Platforms . . . . .	9
2.1.1 Energy supply . . . . .	9
2.1.2 Electric power system . . . . .	14
2.2 The wind turbine technology . . . . .	16
2.2.1 The voltage source converter . . . . .	17

2.3	The Virtual Synchronous Machine . . . . .	19
<b>3</b>	<b>Modeling</b>	<b>23</b>
3.1	System Description . . . . .	23
3.2	The Virtual Synchronous Machine . . . . .	25
3.2.1	Virtual inertia and power control . . . . .	26
3.2.2	SRF voltage and current controllers . . . . .	29
3.3	Wind Turbine Modeling . . . . .	30
3.3.1	Wind turbine converter control . . . . .	31
3.4	Comments on the SRF Controllers . . . . .	32
3.5	Gas Turbine and Synchronous Generator . . . . .	33
3.6	Electrical Load . . . . .	33
3.7	Grid Impedance . . . . .	34
<b>4</b>	<b>Results</b>	<b>35</b>
4.1	Demonstration of Active Load Sharing . . . . .	35
4.1.1	A step-up in active power demand . . . . .	36
4.1.2	Sudden loss of wind power . . . . .	40
4.2	Demonstration of Island Operation Capability . . . . .	42
4.2.1	Operation without gas turbine/SG . . . . .	43
4.2.2	Step up in reactive power demand . . . . .	45
4.3	The Effect of the Virtual Inertia of the VSM . . . . .	45
<b>5</b>	<b>Conclusion</b>	<b>51</b>
5.1	Recommendations for Further Work . . . . .	53
	<b>Appendix A Figures</b>	<b>55</b>
A.0.1	Maturity of wind turbine technology (Source: NVE)[18] . . . . .	55
	<b>Appendix B Screenshots</b>	<b>56</b>
B.1	Screenshot from Simulink of SG parameters . . . . .	56

B.2 Screenshot from Simulink of system overview . . . . .	57
B.3 Screenshot from Simulink of Wind turbine VSC . . . . .	58
B.4 Screenshot from Simulink of Gas Turbine and SG . . . . .	59
<b>Bibliography</b>	<b>60</b>





# Chapter 1

## Introduction

This chapter will introduce the reader to the subject of the report and will cover the motivation for the thesis, the objectives, the scope of work, the limitation, the approach and finally describe the structure of the report.

### 1.1 Motivation

The motivation section of this thesis will be divided into two main parts. The first part will cover the motivation for powering offshore oil and gas platforms with offshore wind. It will discuss how the offshore wind technology might reduce or replace the gas turbines used on the platforms today. The second part will discuss why the VMS might be an applicable technology in this endeavor.

The main motivation for using wind energy to power offshore oil and gas platforms is simply to reduce emissions of harmful gases, such as CO<sub>2</sub> and NO<sub>x</sub>. The challenge of global warming caused by greenhouse emission, represented primarily by CO<sub>2</sub> in this case, is of a great scale. Immense reduction of emissions will have to take place in order to meet the goals of the 2015 Paris Agreement.

According to the environmental report of 2015 [4] from the norwegian oil and gas as-

sociation, the oil and gas industry produced 13.1 million tons of CO<sub>2</sub> in 2014. This is almost one fourth of the total emissions in Norway. The emissions from gas turbines on the platforms stood for 79.4 % of this number. That is 10.4 million tons of CO<sub>2</sub> from the gas turbines alone. These numbers tell us that there is a possibility to largely reduce emissions by phasing out the gas turbines with renewable energy sources.

Another effort to reduce the emissions on the oil and gas platforms is the idea of electrification of the norwegian continental shelf with power cables from shore [18]. This is an effort that has been under way for some years and it is clear to see its link to the offshore wind effort. If offshore wind were to be built, it would need to be linked to shore via cables. One can therefore imagine a future where commercial sized offshore wind farms and oil and gas platforms are linked to the shore with the same grid. This development is discussed in [18], section 10.6 and illustrated in the figure in Appendix A.1 with respect to wind turbine technology (figure is in norwegian). The linking of offshore wind to the platforms is an important step in the development of this infrastructure and will at the same time help reduce the local emissions.

The report [18] argues that the gas turbines on the platforms still would have to run, even if offshore wind power was connected. They need to run in order to maintain the AC frequency, voltage and balance of power, but would be running at a lower power output if offshore wind were to be connected. This will result in a lower efficiency for the turbines which again will lower the reduction of CO<sub>2</sub> emissions. It is therefore of interest to study a technology that would enable the turning off of gas turbines. This would require a power electronic technology that can operate in island operation while maintaining the AC frequency, voltage and power balance. This thesis will study how the "Virtual Synchronous Machine" technology can achieve this. More specifically, it is going to study how a voltage source converter(VSC) that is connected to a battery bank can achieve this by applying a specific control strategy to the VSC. It is this control strategy that will make the VSC behave like a virtual synchronous machine(VSM).

The VSM control approach is expected to be able to operate in parallel with a traditional

synchronous generator (SG), as well as in a converter-dominated environment (island operation). This is possible because it allows for the emulating of the main inherit properties of synchronous machines, namely inertia and damping, as well as being able to define its own frequency.

There is also a third motivational argument to be made and that is the fact that the industry is moving toward this. The powering of offshore platforms by wind turbines is something that is wanted by the industry and there has been large advances in this technology in the latest years. Statoil's Hywind projects are pushing on for floating wind turbines and the technology will most likely be commercially available in the future.

The joint industry project(JIP) named "WIN WIN", led by DNV GL, is another example of the relevancy of the studied technology. The project is looking into the possibility of using a floating wind turbine to power water injection into the reservoirs. The project is showing great results and will hopefully be commercially available in not to long according to [13].

## 1.2 Objectives

This thesis is going to explore the connection of a wind turbine to an offshore oil and gas platform and will use the VSM technology in the process. The following objectives are to be carried out:

1. Design a relevant system to study
2. Build a model of the system
3. Explore the system behavior and identify relevant test cases
4. Simulate said test cases
5. Present and discuss the results

## 1.3 Scope of Work

As stated in the task description, the focus of this thesis is on the VSM's applicability for interfacing wind turbines with offshore oil and gas platforms. The focus will be on how controllers of the different components will interact with each other and what effect they have on load flow and other parameters such as grid frequency.

## 1.4 Limitations

The thesis will cover the control strategies of the various components of the system to a greater extent than the physical components themselves. The modeling of the wind turbine, converters, electrical machines and loads are therefore simplified and often not discussed in detail.

### Limitations in the model

The model that is built in this thesis introduces a set of limitations. Several simplifications have been done when modeling in order to better fit the scope, and to make the modeling easier. The modeling is covered in detail in chapter 3, so this section will cover what limitations the model has, and why it has them.

As mentioned in the scope of work, the modeling of the physical components themselves has not been a priority. The power electronic converters in the model for example, is based on average models. These average models don't take in switching signals as input, but take voltage references instead. The voltage reference inputs represent the average output voltage at the terminals of the converter. The average model of a converter cannot represent harmonics, so harmonics cannot be studied. The average model also assumes the converter to be ideal, which implies that there are no losses in the electronics.

The modeling of electrical loads has been done by simple impedances and not by complex

models of electrical loads such as induction machines. Induction machines are one of the most common motors on offshore oil and gas platforms and are used to power a variety of loads. Contingencies in the system would certainly have an impact on the operation of these motors, but the simplification of the load modeling limits the study of it in this thesis.

The modeling of power from wind turbines are not covered in detail in this thesis; the model does not include actual measured wind data to emulate the power coming from wind turbines. The sea cables from the wind turbine could also have impacts on the system, but they are not modelled in this thesis.

## **Limitations in the studied system**

The power system studied in this thesis is not very complex and has been simplified to a great extent in order to make analysis and simulations easier. This low complexity imposes limitations on how advanced the test cases can be. It also limits the relevancy of the findings to real life cases by making them more theoretical and related to only a small part of an actual system. This is of course all related to the scope of work and a design and analysis of much more complex system would not have been feasible with the time and resources at hand.

The system doesn't contain any infrastructure for reconnecting the VSM to the grid if it initially was running in island operation. The system would need to have a synchronization controller such as the one described in [8] in order to make reconnection possible. The lack of this technology in the system means that scenarios such as synchronization of the VSM with an already operational synchronous generator cannot be studied.

## 1.5 Approach

This master thesis is a continuation of a specializing project[17] that was conducted during the fall of 2015. The work began with a literature search where the goal was to get an overview of the different VSM implementations that exist and to observe what applications it may serve. Further, the search became more focused on one type of VSM implementation, namely the one presented in the papers [10] and [11]. This one was studied in detail and a lot of time was spent on understanding its behavior and how it worked.

A model of this VSM was developed and implemented into the simulation environment called Matlab®Simulink® during the fall of 2015. This model only contained the VSM, a local load and a grid connection possibility. During the fall of 2015, the work on this model was limited mainly to understanding its behavior, and to confirm that the model worked the way it should.

A new model was developed during the winter and spring of 2016. It used the VSM model from the specializing project, but a lot of time went into expanding the model. The new model contains a wind turbine and a gas turbine with a synchronous generator in addition to the VSM, local load and grid connection. The background for, and the development of this model constitutes a large portion of the work for this thesis.

The work on this model continued through the spring of 2016 and the focus was on gaining understanding of the models behavior. This work included the testing of various inputs and altering of parameters to see how the system responded. This work was crucial in order to identify relevant test cases to present and analyze. The simulation, analysis and presentation of these test cases constitutes the final work for this thesis.

## 1.6 Structure of the Report

The thesis is divided into five chapters. First is the introduction, which you are reading now. Then comes chapter 2, which covers the background for the technologies and concepts studied in the thesis. Further we have chapter 3 where the studied system is presented and the modeling of the system is covered. In chapter 4 the results of the simulations are presented and in chapter 5 you will find the conclusions, as well as recommendations for further work.





# Chapter 2

## Background

This chapter will cover the technical background of the various concepts studied in this thesis and will discuss the state of the different technologies.

### 2.1 Traditional Offshore Oil and Gas Platforms

A traditional offshore oil and gas platform is a large structure whose main purpose is to pump up and process hydrocarbons from beneath the seabed. The platforms can also contain facilities to drill wells, as well as storing and transporting the hydrocarbons.

#### 2.1.1 Energy supply

The main power source of a traditional offshore oil and gas platform is gas turbines. This is a natural choice given the availability of the fuel at the platforms. The turbines also have a low weight and compact size relative to its power output which is beneficial when considering the space and weight limitations of an offshore platform. It is common to have at least two or three gas turbines on a platform. It is also common to have a diesel generator and a UPS system for emergency power systems, but in the background of

this thesis we will mainly focus on the gas turbine as a prime mover of a synchronous generator.

The power coming from the prime mover is regulated by a *governor*. The purpose of this controller is to regulate the valve which supplies the turbine with its fuel. It measures the speed at the axel, as depicted in figure 2.1, and strives to keep the axel rotating at the speed reference set point. There are various control schemes that exist for governors, but here the focus will be on a simple frequency droop controller. This control scheme can be seen in the block diagram of figure 2.4. This model is simplified and has neglected the time delay of a servomotor and the behavior of the turbine. With these simplifications, the actions of the prime mover can be expressed by equations (2.1) and (2.2).

$$p_m = p_{ref} + \frac{1}{\rho} \cdot (\omega_{ref} - \omega_{sync}) \quad (2.1)$$

Here,

- $\rho$  is the *frequency-droop-characteristic* of the governor (defined by equation (2.2)),
- $p_{ref}$  is the power reference,
- $p_m$  is the mechanical power provided by the prime mover,
- $\omega_{ref}$  is the speed reference set point,
- $\omega_{sync}$  is the synchronous speed,

These parameters are all in per unit, hence the lower case lettering.

$$\rho = -\frac{\Delta\omega}{\omega_n} \cdot \frac{P_n}{\Delta P_m} \quad (2.2)$$

Here,

- $\omega_n$  is the nominal speed of the machine
- $P_n$  is the nominal power of the machine

- $\Delta\omega$  and  $\Delta P_m$  is the change in speed and mechanical power, respectively.

The *frequency-droop-characteristic* of the synchronous machine is important, not only to frequency control, but to the sharing of load between generators in parallel operation [20]. The different droops of the governors will determine how large share of the load will be covered by each power source. It will also determine the electrical frequency of the grid in question. Both these concepts are illustrated in figure 2.2. This figure is sometimes called a "house diagram" and the droop for the generators correspond to the slope of the "roof". The scenario depicted is not connected to the power grid, which implies that the two generators G1 and G2 need to cover the total load. If the load is changed, then the slope of the curve of the two generators will determine how the additional load is distributed between the two; the system frequency named  $f_e$  in figure 2.2 has to be equal for the two generators.

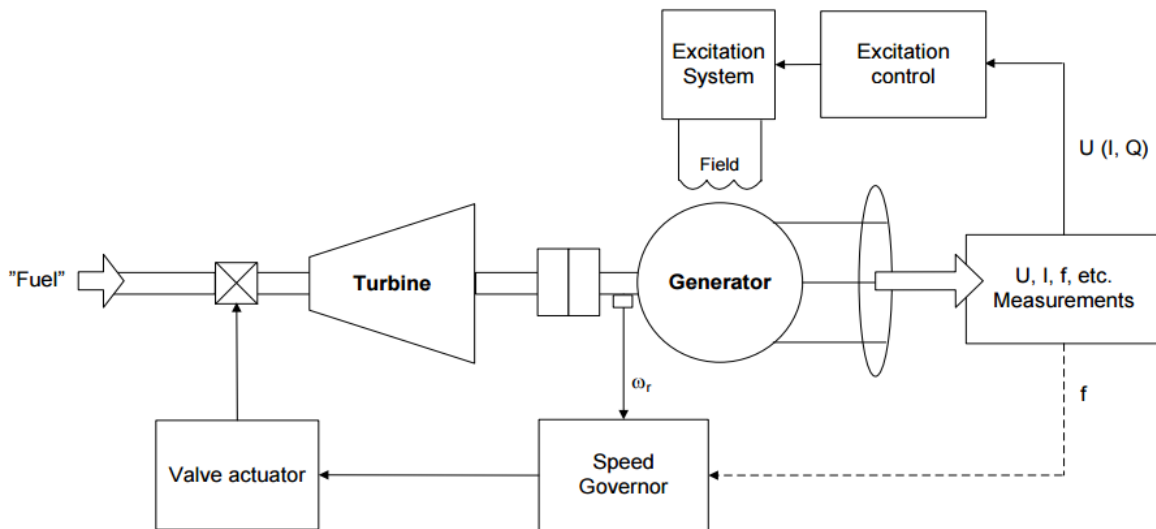


Figure 2.1: Turbine and Generator [21]

The starting position of the curves on the y-axis is determined by the governor set points or the active power reference of the controller. This is the same as  $p_{ref}$  in equation (2.1). Increasing the active power reference for one generator would displace its curve in

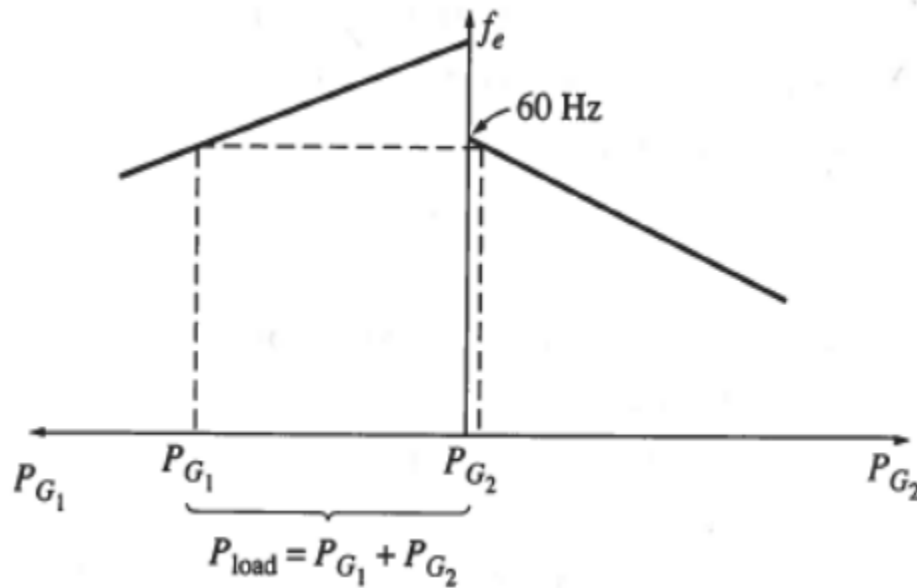
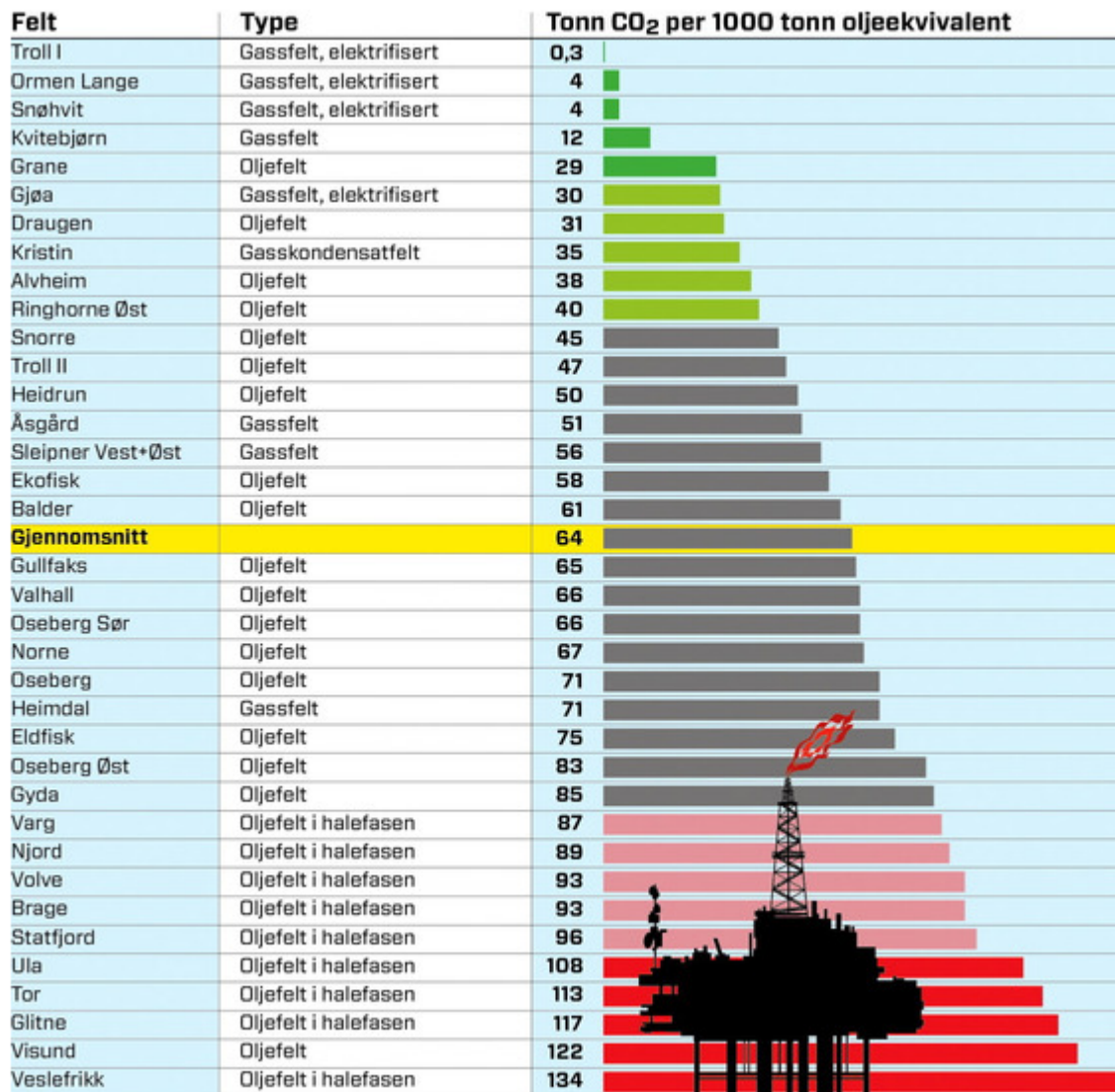


Figure 2.2: House diagram for load sharing [20]

the positive  $y$  direction. This would again result in an increased system frequency and increase the power supplied from that generator while the power from the other would decrease.

In recent years there has been a development towards powering offshore platforms with cables from land instead of using the gas turbines, with the goal of reducing greenhouse emissions [18]. Figure 2.3 (figure is in norwegian), which has its data from [12], shows how the gas fields that get their power from shore generally has the lowest CO<sub>2</sub> per oil equivalent and that the oil fields in the tail phase of their lifetime has the highest. The oil and gas fields on the norwegian continental shelf are often viewed as already having low emissions, but this graphic indicates that there is a lot of potential in CO<sub>2</sub> emission reduction when it comes to the fields in the tail phase. The oil fields in the tail phase are also the ones in greater need of water injection to achieve improved oil recovery (IOR) which makes the previously mentioned DNV GL JIP named "WIN WIN" highly relevant to these fields.

Figure 2.3: CO<sub>2</sub> emissions from platforms on the norwegian continental shelf [19]

### 2.1.2 Electric power system

Electric power generation on a traditional offshore platform is done by a synchronous generator powered by the gas turbines previously covered. The synchronous generator has several static and dynamic properties that the grid on the platform rely on to operate. These properties are primarily the inertia and damping of the machine.

The inertia of the synchronous machine is provided by its rotating machinery. This rotation machinery includes the rotor of the machine and the rotating parts of the turbine which is connected to the rotor via an axle. This is illustrated in figure 2.1. It is also possible to connect a flywheel to the rotor in order to provide additional inertia.

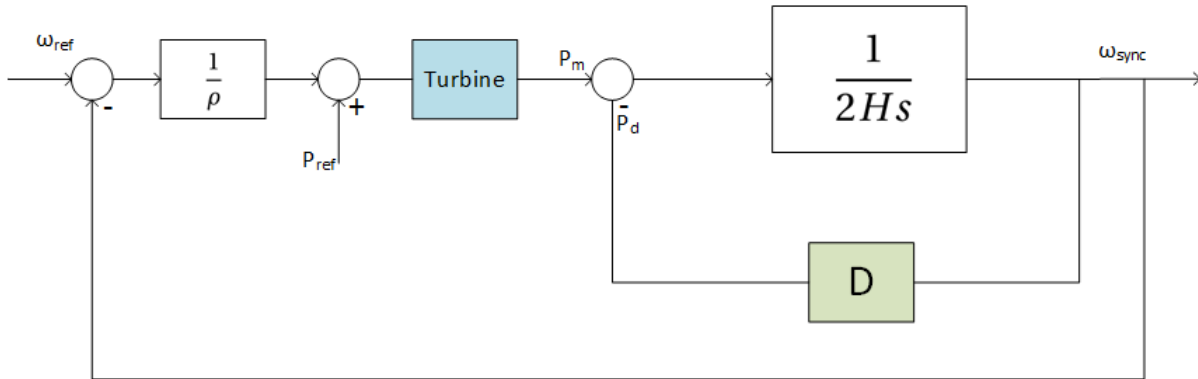


Figure 2.4: Block diagram of a synchronous machine and turbine

The rotational motion of the synchronous generator is described by equation (2.3). This equation is called its "swing equation" and is based on newton's second law of rotation. The block diagram of this equation can also be seen on the right side in figure 2.4. This figure also illustrates the governor and prime mover on the left side.

$$2H \frac{d\omega_{sync}}{dt} = p_m - p_e - p_d. \quad (2.3)$$

Here,

- $H$  is the normalized inertia constant
- $\omega_{sync}$  is the synchronous angular speed of the machine

- $p_m, p_e$  and  $p_d$  is mechanical-, electrical- and damping power, respectively.

The normalized inertia constant  $H$  is in the units of seconds. It describes how much kinetic energy is stored in the rotating machinery at the speed  $\omega_{sync}$ . When normalized, it gives the number of seconds it would take the generator to provide the electrical energy equal to the amount stored in the rotating machinery when operating at its rated apparent power [16]. In other words, the inertia constant gives us information about how the rotating speed of the machine will be affected by change in the electrical power. It is also common to use the mechanical time constant  $T_a$  to describe the inertia, in which case  $T_a = 2H$ .

The mechanical power  $p_m$  is the power provided by the prime mover, which in this case is the gas turbine. The damping power  $p_d$  is mainly provided by the damper windings in the rotor poles. These windings will get an induced current when there is a difference between the mechanical speed of the rotor, and the speed of the magnetic field set up by the current in the stator. The current in the damper windings will set up a field which will try to restore the speed of the rotor. If we simplify further and assume no leakage flux and neglect resistance in the damper windings we can describe the damping power with equation (2.4).

$$p_d = D \cdot (\omega_m - \omega_{sync}) \quad (2.4)$$

Here,  $\omega_m$  is the mechanical speed and  $D$  is the damping coefficient of the machine.

The excitation control seen in the top of figure 2.1 controls the field current in the rotor windings. Its task is to regulate the voltage magnitude of the induced voltage in the stator by regulating the rotor field magnitude. This voltage magnitude can be regulated based on several different schemes with the goal of controlling either the line voltage or the reactive power production of the machine. The excitation of the synchronous machines in this thesis will be voltage controlled and the scheme will not be studied in detail.

## 2.2 The wind turbine technology

The wind turbine technology has advanced immensely the last three decades. In 1985 the wind turbines had rotors that were 15 meters in diameter and produced less than 1 [MW] of power. Today the average onshore wind turbine produces between 2.5 and 3 [MW] and has rotor diameters over 100 meter. The largest turbines however, can produce up to 7.5 [MW] and have rotors that are over 120 meters in diameter[3]. MHI Vestas offshore wind's V164-8.0 MW® prototype turbine also sat a new record for wind energy production when it produced 192.000 [kWh] in 24 hours in 2014.

Conventional offshore wind turbines that are mounted on the seabed has also been around for some time now and there are many operational offshore wind farms in the North sea. Take the norwegian owned Sheringham Shoal offshore wind farm for instance. It is located off the east coast of the UK in depths ranging from 17-22 meters and produced 484.29 [GWh] in 2012 [1].

According to [18], the most likely connection of wind farms to offshore installations in short term would be near the oil fields in the southern part of the North sea. In this area of the North sea the water is 60-90 meters and the mounting of wind turbines on depths of 60 meters might be possible in the near future.

Another promising, but more long term technology is the floating wind turbine. This technology is not yet commercially available, but has larger applicability towards offshore platforms since deeper waters will be accessible. The Hywind Scotland Pilot Park by Statoil for instance, will be mounted on depths up to 120 meters [2] and the formerly mention "WIN WIN" JIP led by DNV GL is focusing on floating wind turbines and the possibility of using it for water injection into reservoirs.



### 2.2.1 The voltage source converter

In this thesis, voltage source converters will be applied in two areas. The first application is to connect the wind turbines to the electrical grid on the platform, and the second application will be the interface with a battery storage unit. The latter will be controlled as a virtual synchronous machine and the combination of the VSC and battery may sometimes be referred to as simply "the VSM".

A voltage source converter is a power electronic device used to convert DC to AC (inverter mode) or AC to DC (rectifier mode). The VSC use transistors, usually the insulated-gate bipolar transistor (IGBT) in parallel with diodes to achieve self-commutation. The IGBT is controlled by a signal which enables the closing or opening of the IGBT switch.

The wind turbine connection studied in this thesis is that of a back-to-back connection, which is two VSC's connecting two AC-grids together via a DC link. This enables variable frequencies on the two sides of the converters, something that is crucial for the optimal operation of the wind turbines. This technology also makes it possible to use permanent magnet synchronous generators(PMSG) as opposed to the technology using doubly-fed induction generators(DFIG). The PMSG tend to cost more, but it is more efficient than the DFIG, and more compact than the regular wound rotor synchronous generator. The PMSG is also more reliable than DFIG; all these factors are making PMSG and back-to-back VSC's favorable for offshore use [6].

#### Operation and control of the VSC

The operation of the VSC's is done through the concept of pulse-width-modulation(PWM). This involves comparing a control signal with a saw-tooth signal to provide "on or off" orders to the IGBT/diode blocks of the VSC. However, this thesis will not focus on the switching operation of the VSC, but rather on the controller of the VSC.

Both the controllers of the VSM and the VSC of the wind turbine apply a rotating

synchronous reference frame; the controllers are often referred to as synchronous reference frame controllers or SRF controllers. The values of current and voltage on the AC side of the VSC is measured in the three phases a, b and c. This is the abc-reference frame, which is a stationary one. These measurements pass through a park/clark transformation and end up in a rotating dq-reference frame. The park/clark transformation takes an angle as input and use it as a frame of reference. This angle can for example be the electrical angle of the grid voltage and will be rotating depending on the grid speed. The reference frame set up by the park/clark transformation will therefore be rotating with the speed of its reference angle. In the model used in this thesis, the d-axis is parallel to the vector a, and the q-axis leads the d-axis by 90 degrees. This rotating reference frame enables the use of simple PI controllers for controlling the voltage and current. Note that the voltage also can be measured at the DC side of the VSC if that is the voltage you wish to control.

The current and voltage controller of a VSC consists of one inner and one outer control loop. The inner control loop, depicted in figure 2.5, strives to keep the output current equal to the reference current with the use of feedback of the measured output current, and a PI controller. Figure 2.5 also shows how the measured current values  $I_{abc}$  passes through park/clark transformation block in order to be compared with the reference value  $I_{dq,ref}$ . The park/clark transformation will need a reference angle and it is normally is provided by a phase locked loop which measures the angle of the AC grid.

The outer loop, seen in figure 2.6, has the same layout as the inner loop, with a feedback through a park/clark transformation and a PI controller. The output of the voltage PI controller is the reference current of the current controlling inner loop.

The tuning of these controllers is a challenge in itself and will not be covered in this thesis. A common approach is the modulus optimum tuning method for the inner current loop and the symmetrical optimum for the outer voltage loop. It is also important to make sure that the time constants of the two controllers don't overlap, so that they don't work against each other.

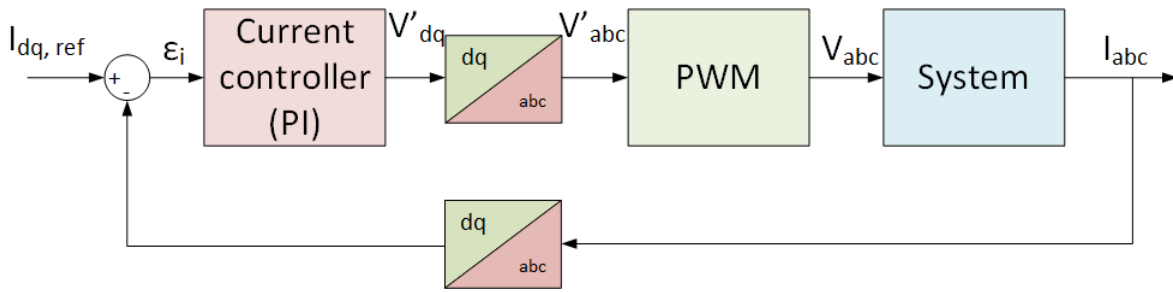


Figure 2.5: Inner control loop

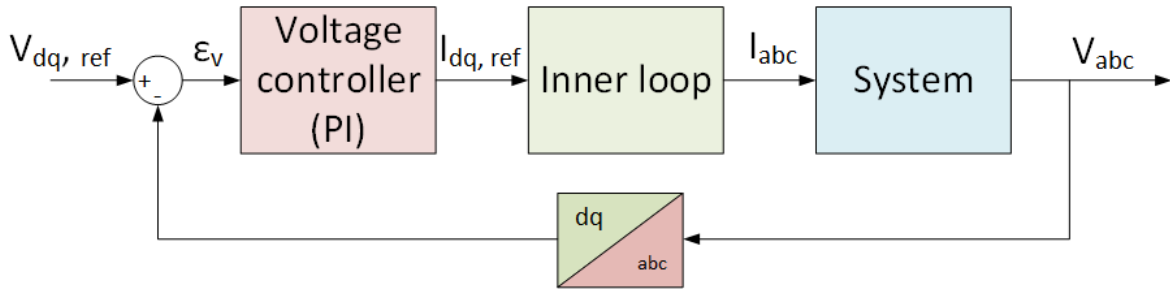


Figure 2.6: Outer control loop

## 2.3 The Virtual Synchronous Machine

The concept of a Virtual Synchronous Machine was first presented in [5]. The paper uses the abbreviation "VISMA", while this thesis will use "VSM". The original application for the VSM was for use in distributed energy sources. As discussed in [17], the traditional power system has a vertical structure with power production in one end and consumption in the other. The large, centralized power plants of the traditional power system use synchronous machines for electric power generation. The synchronous machine possess several important parameters such as inertia and damping that are crucial for the operation of a power system. These are further described in section 2.1.2. However, the power system is moving toward more distributed energy sources, such as photovoltaics (PV) and local energy storage. The connection of these sources to the grid is achieved through the use of power electronics such as VSC's. A distributed power source that is connected to the grid with a VSC doesn't introduce properties such as inertia and damping of which the power system relies on. The idea of the VSM is therefore to control the VSC in such

a way that it mimics the behavior of a synchronous machine, and in that way provide the properties of damping and inertia that the power system is wanting.

The VSM presented in [5] applies a 7<sup>th</sup> order model of a synchronous machine which provides current vector references to the controllers of the VSC. It models both the swing equation of the rotor and the excitation of the rotor field to full extent, meaning that it has both virtual inertia and excitation similar to that of an actual synchronous machine. The paper [5] concludes that the method presented will enable connection of distributed energy sources to weak grids via VSC technology without altering the operation of the grid.

Following the first VISMA paper [5], several new approaches to VSM's emerged. Their goals often being to simplify the modeling of the virtual machine, applying different control strategies or to explore applications of the technology. The paper [7] presents an overview of the different VSM implementations that has emerged up until 2013. The variations extend to the use of different references, model orders and application of controllers.

The VSM implementation used in this paper is based on the one described in the papers [10] and [11]. However, that implementation is an expansion of the one used in [9], where the layout with an outer loop is applied for inertia emulation. This outer loop emulates a simplified 2<sup>nd</sup> order swing equation of a synchronous machine, as well as a droop-based reactive power controller, which provides voltage references to cascaded voltage and current controllers (SRF controllers). A further description of the inertia emulation, reactive power controller and cascaded voltage and current controllers will be presented in chapter 3.

The implementation of the VSM in [10] and [11] is similar to the one in [9], but now the swing equation and reactive power controller gives a voltage reference to a virtual impedance which adds a voltage drop to the voltage reference proportional to the output current of the VSC, before providing the reference to the cascaded voltage and current controllers (SRF controllers). The virtual impedance behaves, in other words, as an impedance would, by measuring the output current of the VSC and changing the voltage

reference accordingly. The virtual impedance is important when operating in resistive grids, such as in island operation since it helps to decouple the active and reactive power. The virtual inductance also helps with reducing the VSM's sensitivity to small signal disturbances by introducing an angle displacement between the grid voltage and the virtual inertia position.



# Chapter 3

## Modeling

In this chapter you will find a description of the analyzed system, as well as a description on how it has been modeled.

### 3.1 System Description

The studied system, seen in figure 3.1, is representing a simplified power system of an oil and gas platform with wind power and a battery bank. It consists of:

1. A wind turbine
2. A battery bank with a VSC (operated as a VSM)
3. A synchronous generator powered by a gas turbine
4. A Local load
5. The possibility of a stiff grid connection.

The system has an option to connect to the grid. This is not a part of any real system since it is supposed to be a grid on an oil and gas platform miles from shore. It is included to reach steady state faster during simulations. The stiff grid is thus disconnected before

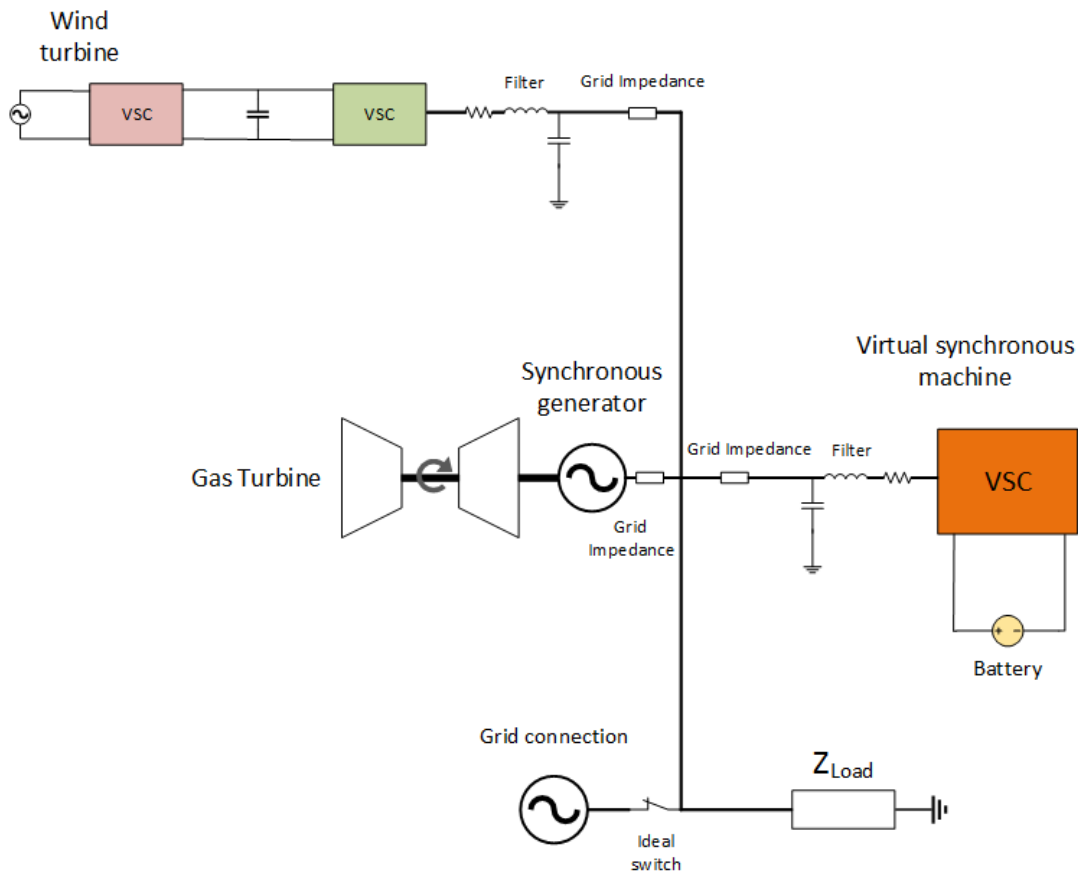


Figure 3.1: One line diagram of the system

any scenarios related to the test cases occur.

It is normal to have more than one gas turbine on an oil and gas platform, but it has been simplified into one turbine since the parallel operation of two regular SG's is outside the scope. A real system would also contain transformers and loads on different voltage levels, but this has been simplified and the load is concentrated as one impedance at the same voltage level as the production. The loads and power sources are not intended to represent realistic power consumption on oil and gas platforms in terms of size. The voltage level is also different than it might be in a real system. This is why the results will be presented in per-unit.

All the components are connected to an AC-bus with rated voltage  $U_n = 690[V]$  and frequency  $f_e = 50[Hz]$ . Both the VSM, wind turbine and the synchronous generator has



the same apparent power base  $S_b = 2.7488[MW]$ . The base value for specifying voltages in per unit is set to be the peak of the phase voltage. This entails that

$$U_{ACbase} = \sqrt{\frac{2}{3}} \cdot U_n = 563.4[V] \quad (3.1)$$

for the AC part of the system, and

$$U_{DCbase} = 2\sqrt{\frac{2}{3}} \cdot U_n = 1126.8[V] \quad (3.2)$$

for the DC link. A system overview can be seen in figure 3.1 and a screenshot of the Simulink implementation can be seen in appendix B.2.

## 3.2 The Virtual Synchronous Machine

The figure 3.2 shows the topology of the VSM and how it has been connected to the rest of the system.

As mentioned in chapter 2, the VSM in this thesis is based on the one described in [10] and [11]. The battery bank that is powering the VSM is implemented as a DC voltage source to simplify the model. An average model is applied to represent the VSC itself. This model is found in the Simulink® Simscape Power Systems™ library. This implementation will not cause any switching ripples as opposed to the PWM and IGBT implementation. The difference between these implementations has been discussed in the specializing project that precedes this thesis [17], and it was found that the average model was sufficient when not studying the effects of the switching ripple and it removed distortions in the output power, making it easier to study the power from the VSM. However, as discussed in the limitations, this means that the effects of these harmonics won't be observed.

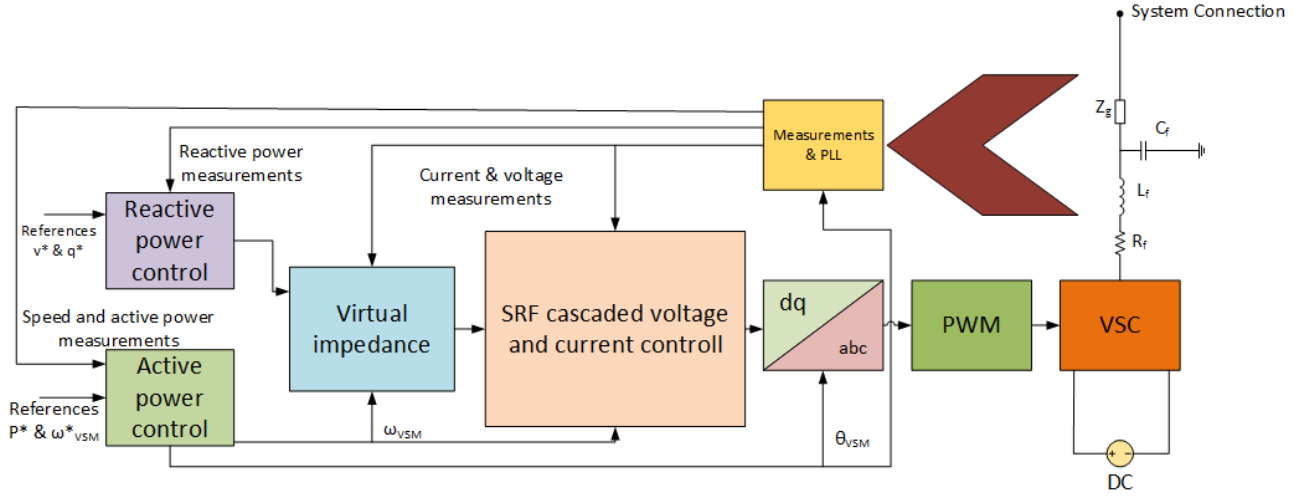


Figure 3.2: VSM topology

### 3.2.1 Virtual inertia and power control

The active power control of the VSM, located in the bottom left corner of figure 3.2, is based on the behavior of a synchronous machine's swing equation, as well as its governor. The swing equation in question was introduced in chapter 2 and is described by equation (2.3).

The damping power, which has been simplified to equation (2.4), will be changed to equation (3.3) for the VSM. The speed  $\omega_{PLL}$  is the measured electrical speed at the AC side of the VSC. This speed is measured with the use of a phase locked loop (PLL). The PLL used in this model is based on [14] and [15]. This is the same as the PLL used in [10] and [11]. An identical PLL is also used for the control of the VSC of the wind turbine.

$$p_d = k_d \cdot (\omega_{VSM} - \omega_{PLL}) \quad (3.3)$$

Here,

- $p_d$  is the damping power in per unit,
- $k_d$  is the damping coefficient,

- $\omega_{VSM}$  is the virtual speed,
- $\omega_{PLL}$  is the measured PLL speed.

In the VSM, the mechanical power  $p_m$  from the prime mover has been replaced with a virtual mechanical power. This power is defined by equation (2.1) and is the sum of the reference power and the signal from the governor. In this thesis a traditional frequency droop controller is used.

$$p^{r*} = p^* + k_\omega \cdot (\omega_{VSM}^* - \omega_{VSM}) \quad (3.4)$$

Here,

- $p^{r*}$  it the virtual mechanical power,
- $p^*$  is the active power reference,
- $\omega_{PLL}^*$  is the reference speed,
- $k_\omega$  it the proportionality constant of the controller.

The constant  $k_\omega$  is the same as the inverse of the droop constant from equation (2.2).

The VSM models the electrical power in the stator windings simply by measuring the electric power output from the VSC. This value reflects the electric power drawn from the virtual rotating machinery of the VSM and is represented as  $p$  in equation (3.5).

When combining equation (2.1), (3.3) and (2.3) we get equation (3.5), which is the swing equation that describes the virtual inertia and power control of the VSM.

$$\frac{d\omega_{VSM}}{dt} = \frac{p^*}{T_a} - \frac{p}{T_a} - \frac{k_d \cdot (\omega_{VSM} - \omega_{PLL})}{T_a} + \frac{k_\omega \cdot (\omega_{VSM}^* - \omega_{VSM})}{T_a} \quad (3.5)$$

Here,  $T_a$  is the time constant representing the normalized inertia constant 2H.

The rotor angle  $\theta_{VSM}$  can be found with the use of equation (3.6).

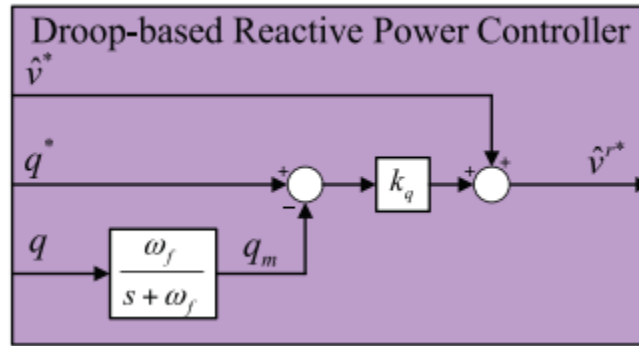


Figure 3.3: Droop-based reactive power controller [10]

$$\frac{d\theta_{VSM}}{dt} = \omega_{VSM} \cdot \omega_b \quad (3.6)$$

The reference speed  $\omega_b$  of this system is set to  $2\pi \cdot 50 \frac{rad}{sec}$ . The values of the various parameters used in the above equations are listed in table 3.1. These are the same values that were used in [11].

Table 3.1: Parameter values of the VSM

Parameter	Value [p.u]
$k_d$	400
$k_\omega$	20
$T_a$	20
$k_q$	0.2
$\omega_f$	1000

### Reactive power and voltage control

The reactive power controller seen on the upper left part of figure 3.2 is illustrated with more details in figure 3.3. This controller is equal to the one in [10] and [11] and is a simple droop-based controller similar to what is used in governors. This block diagram can also be described by equations (3.7) and (3.8). The former describes the actual droop-based reactive power controller, while the latter describes the low pass filter.

$$\hat{v}^{r*} = \hat{v}^* + k_q \cdot (q^* - q_m) \quad (3.7)$$

$$\frac{dq_m}{dt} = -\omega_f \cdot q_m + \omega_f \cdot q \quad (3.8)$$

Here,

- $k_q$  is the reactive power droop gain,
- $\omega_f$  is the cut-off frequency of the low pass filter,
- $\hat{v}^*$  is the voltage magnitude reference,
- $q^*$  is the reactive power reference,
- $q$  is the measured reactive power output in per unit,
- $\hat{v}^{r*}$  is the output voltage reference magnitude that will be sent to the virtual impedance.

The value  $q$  passes through a low pass filter described by equation (3.8), before it is sent to the droop controller as the value  $q_m$ .

The values of the various parameters are listed in table 3.1.

### 3.2.2 SRF voltage and current controllers

The SRF voltage and current controllers of the VSM, sometimes referred to as cascaded voltage and current controllers can be seen in the center of figure 3.2. They operate in the rotating dq-reference frame which makes it possible for the controllers to be of a simple PI type. The outer-loop voltage controller receives its reference via the virtual impedance and provides a current reference to the inner-loop current controller. The current controller then gives a voltage reference in the dq-reference frame. This reference passes through an inverse park/clark transformation which converts the signal to the

abc-stationary reference frame. The transformation uses the angular position  $\theta_{VSM}$  from equation (3.6). In this way, the frequency of the voltage from the converter is provided by the swing equation of the VSM. This voltage reference can then be sent to the PWM, as illustrated in figure 3.2. In this model however, the voltage reference is sent directly to an average model of the VSC.

The SRF voltage and current controllers used in this thesis is equal the ones used in [11] and [10]. The PI controller of the current loop has been tuned with the use of the modulus optimum method and the outer voltage loop applies the symmetrical optimum method for its PI controller. Note that the tuning of said controllers was not performed as a part of this thesis. The VSM implementation used in this thesis is based on the one described in [11] and [10] and the same PI controller settings are used.

### 3.3 Wind Turbine Modeling

In this thesis the modeling of the wind turbine has been largely simplified. The studied wind turbine is connected to the rest of the grid with two back to back VSC's, but since the focus of this thesis is on the electric grid, and more precisely the AC grid of the system, several simplifications has been done. The wind turbine has been modeled as a variable DC-current source in parallel with a capacitor. This is again connected to the system with a VSC. This simplification is illustrated in figure 3.4. Just like the VSM, the VSC of the wind turbine is implemented using an average model so the ripple caused by the PWM switching is removed. The Simulink implementation of this can be seen in appendix B.3.

The filter between the wind turbine and the system connection is identical to the one of the VSM, but it is not included in figure 3.4. Neither of these filters are discussed in detail since harmonics aren't studied.

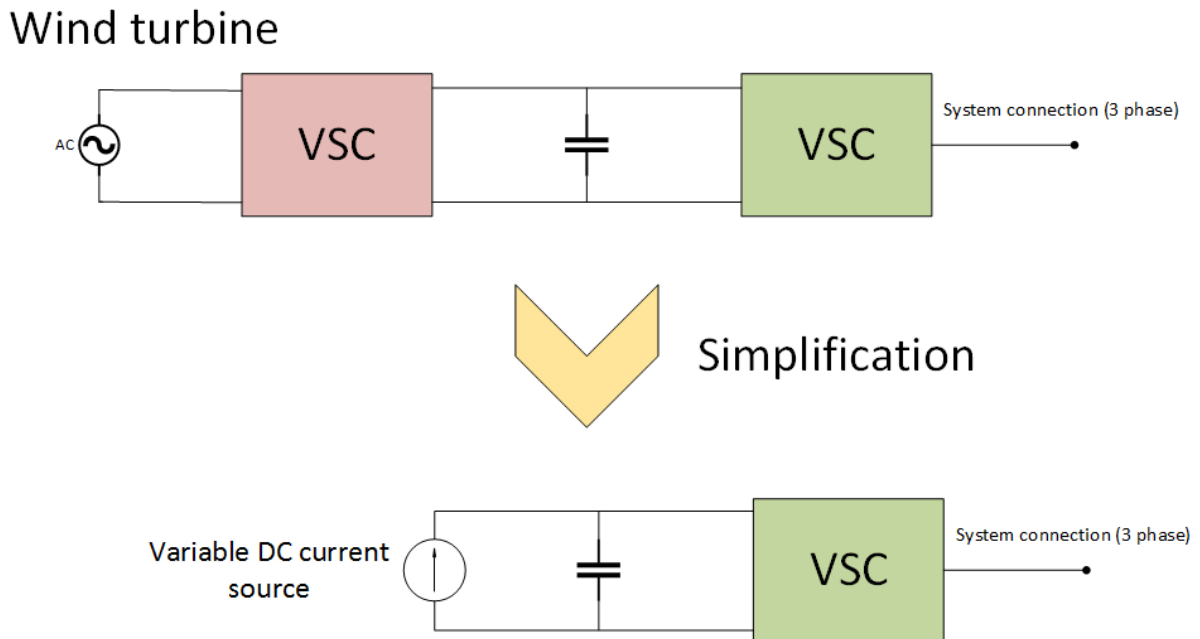


Figure 3.4: Simplification of wind turbine

### 3.3.1 Wind turbine converter control

The current and voltage controller of the wind turbine converter has a similar layout as the voltage and current controllers of the VSM. It is operating in the rotating dq-reference frame which enables the use of simple PI controllers. This rotating frame however, gets its reference angle for the park/clark transformation from the grid speed with the use of a PLL. As opposed to the VSM which uses its own swing equation to provide the reference angle.

The inner loop current controller is identical to the one used in the VSM. No reactive power control has been implemented for this converter so the q reference current is set to be zero. The d current reference however, is given by the DC voltage controller as seen in figure 3.5. This is a simple PI controller which takes in the difference between the DC voltage reference and the measured DC voltage. This DC voltage is measured at the capacitor that is seen in figure 3.4.

It is worth mentioning that the signal coming from the controller, seen on the right side

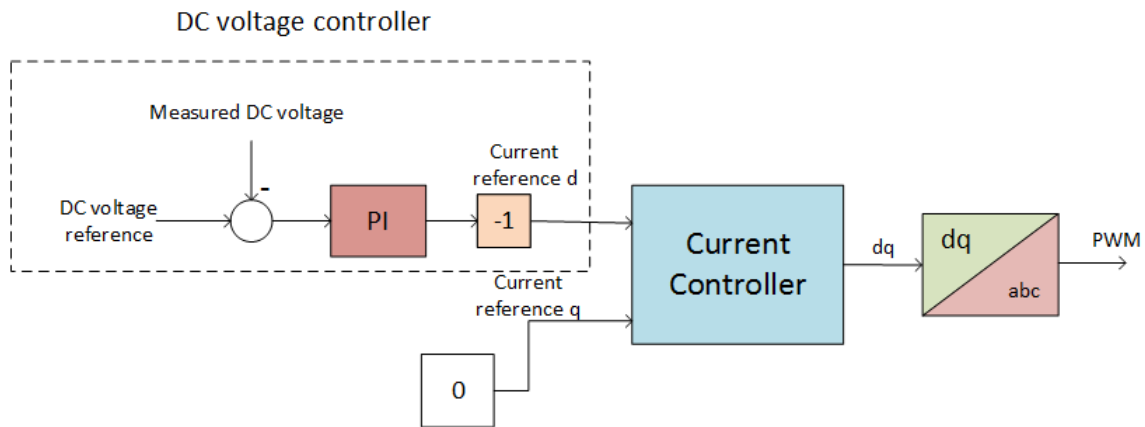


Figure 3.5: Control of wind turbine VSC

of figure 3.5 is to pass through a PWM that would control the switching of the VSC. This is not the case however, since an average model has been used for this thesis.

### 3.4 Comments on the SRF Controllers

The difference between the park/clark transformation of the VSM and that of the wind turbine converter is that the VSC uses its own internal angle and speed for the transformation, while the wind turbine converter uses a phase-locked loop (PLL) to keep track of the electrical speed of the grid. The rotating reference frame of the VSM is in other words based on its own speed, while the wind turbine reference frame is based on the grid speed. This is what enables the VSM to have its own torque angle and speed which is provided by its swing equation.

It is also important to note that the SRF voltage controller of the wind turbine is controlling the voltage on the DC link, while the same controller for VSM controls the voltage on the AC side of the VSC.



## 3.5 Gas Turbine and Synchronous Generator

As discussed in the scope of work, the physical components of the system in not studied in detail. This extends to the modeling of the gas turbine. This thesis will not cover the dynamic properties of the turbine and the power input to the generator is therefore being fed directly from a simple governor. The synchronous generator itself is also not studied and a pre-made model from the Simulink® Simscape Power Systems™ library is therefore utilized. This also includes the excitation system of the generator which regulates the voltage magnitude. A screenshot of this implementation from Simulink® can be found in appendix B.4.

The pre-made model of the SG is of a round rotor type. It has the same power rating as the other components in the grid,  $S_b = 2.7488MVA$ . Its steady state, transient and sub-transient parameters, as well as its inertia constant  $H$  can be found in appendix B.1. The implication of these values are not discussed in this thesis.

## 3.6 Electrical Load

The local electrical load of the platform is modeled as a star-connected impedance with the possibility to connect an additional, identical impedance in star-connected parallel. This additional impedance would effectively double the load (assuming the voltage remains unchanged). The value of the impedance is listed in table 3.2. This impedance would consume 0.5 [p.u] of active power under normal conditions.

Table 3.2: Impedance values of the electric load

Parameter	Value
$r_{load}$	2 [p.u]
$l_{load}$	0.2 [p.u]
$R_{load}$	0.3464 [ $\Omega$ ]
$L_{load}$	0.1103 [mH]

### 3.7 Grid Impedance

The wind turbine, VSM and SG has, as you can see in figure 3.1, a grid impedance between themselves and the point of common coupling (PCC). This impedance represents the resistance and inductance in the line between the component and the PCC. The resistance and inductance values are equal in the three cases and listed in table 3.3.

These impedances would not be equal in a real scenario but it was chosen this way for the sake of simplicity. There would also be sea cables from the wind turbine to the platform to further complicate the modeling.

Table 3.3: Grid impedance values

Parameter	Value
$r_{grid}$	0.01 [p.u]
$l_{grid}$	0.2 [p.u]
$R_{grid}$	0.0017 [ $\Omega$ ]
$L_{grid}$	0.1103 [mH]

# Chapter 4

## Results

This chapter will present the results of various simulations performed in Matlab®Simulink®. The simulated events will attempt to represent realistic scenarios related to the operation of the system described in chapter 3. The goal is to demonstrate and explore the various properties and capabilities of the VSM, as well as its practical suitability. This is done by studying the system's behavior during several scenarios.

All the values presented in plots in this chapter will be in per-unit.

### 4.1 Demonstration of Active Load Sharing

This section contains results from simulation scenarios whose primary objective is to demonstrate how the active load is distributed between the various components in the system during different events. It is important for the practical suitability of the VSM to see how it performs in parallel to a synchronous generator.

### 4.1.1 A step-up in active power demand

In this scenario there will be a step-up in the electrical load by connecting an additional impedance in parallel. This results in a near doubling of the active electrical load at  $t = 6.5[s]$  and can be seen in figure 4.2. The parameters of interest are listed in table 4.1. The wind turbine is set to produce a constant 0.25 [p.u]. This means that the wind turbine and the gas turbine can cover the initial load without the help of the battery bank. Setting the power references of the gas turbine and VSM to 0.25 [p.u] and 0 [p.u] respectively, will cause the speed to be nearly 1 [p.u] before the load is increased. This is also the reference speed for all the controllers in the system.

Table 4.1: Test case 1.1: Parameter values

Parameter	Value [p.u]
$p_{VSM}^*$	0
$k_{\omega VSM}$	20
$p_{sync}^*$	0.25
$k_{\omega sync}$	30
$\omega_{ref}$	1

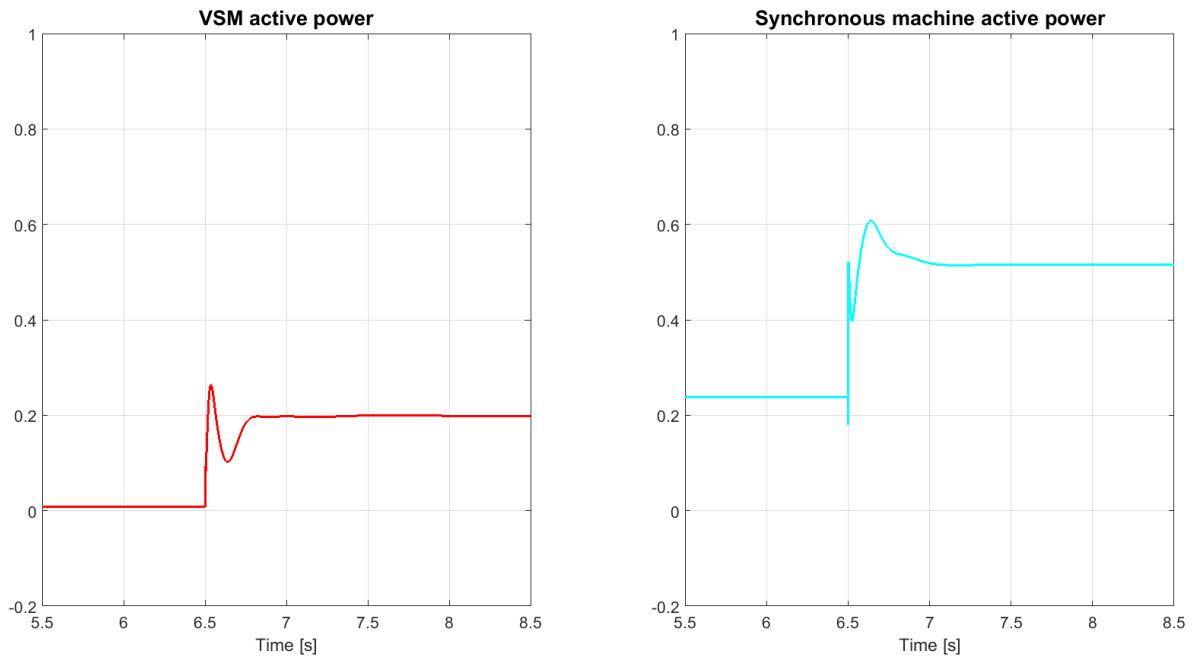


Figure 4.1: Test case 1.1: Active power a)

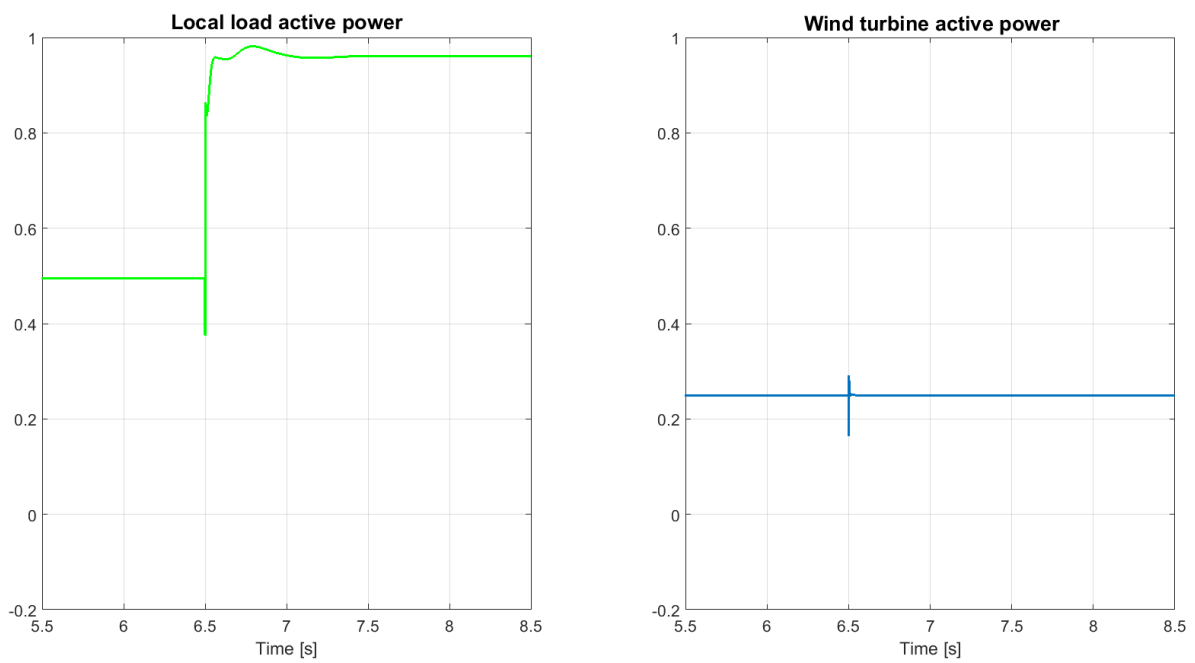


Figure 4.2: Test case 1.1: Active power b)

Observe figure 4.1 and 4.2. It shows how the initial load is covered by the wind turbine and the SG from  $t = 5.5[s]$  to  $t = 6.5[s]$ . When  $t = 6.5[s]$ , the additional load is added and we get a transient period before steady state is reached around  $t = 7[s]$ . The synchronous machine and the battery bank are now sharing the increased load between themselves. The sharing of load is determined by the constants  $k_{\omega VSM}$  and  $k_{\omega Sync}$  of the power controllers. These constants are, as mentioned in section 3.2.1, the same as the inverse of the droop constant  $\rho$ .

When neglecting the grid losses and the losses in the SM, we get equation (4.1), which can be combined with equation (2.1) to calculate the new synchronous speed of the system; the calculations can be seen in equation (4.2).

$$p_{load} - p_{wind} = p_{VSM} + p_{sync} \quad (4.1)$$

$$\omega_{sync} = \frac{p_{refVSM} + p_{refSync} - (p_{load} - p_{wind}) + \omega_{ref} \cdot (k_{\omega VSM} + k_{\omega Sync})}{k_{\omega VSM} + k_{\omega Sync}} = 0.99 \quad (4.2)$$

This calculated value matches the plot of the measured speed in figure 4.3. That is, after steady state is achieved at  $t = 7[s]$ . By applying this speed to equation (2.1) one gets a new VSM power of 0.2 [p.u]. This corresponds to what we see in figure 4.1 after  $t = 7[s]$ .

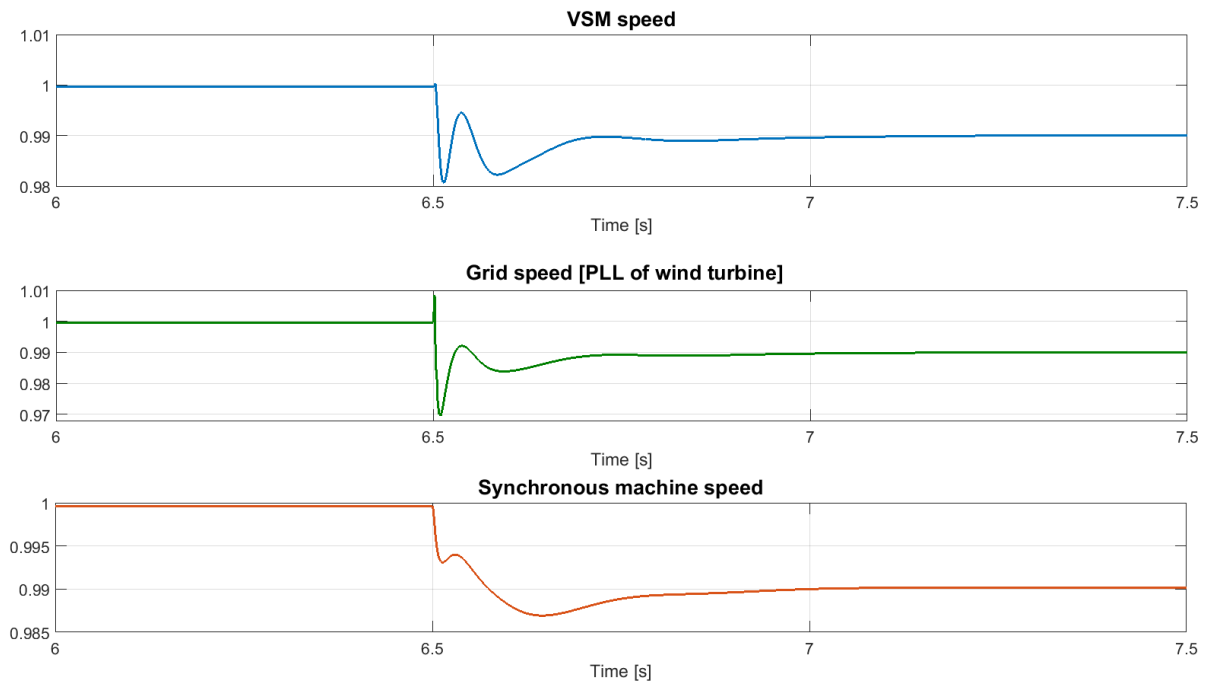


Figure 4.3: Test case 1.1: Various system speeds

### Scenario without the battery bank

Figure 4.4 shows speeds of the system when it is subjected to the same scenario as before, only this time without the support of the VSM operated battery bank, which has been disconnected from the system. It is just the SG and the wind turbine that is supporting the load. This means that when the additional load is added at  $t = 6.5[s]$ , the SG needs to cover that increased load by itself. What this shows is that the initial drop in grid speed measured by the wind turbine PLL is larger than when the battery bank was included in the system, seen in figure 4.3. This indicates that the VSM is introducing inertia into the system and reducing the initial drop in grid speed.

You can also see how the speed after  $t = 7[s]$  is lower than in the previous case. The speed is now determined only by the governor of the SG and not the VSM of the battery bank.

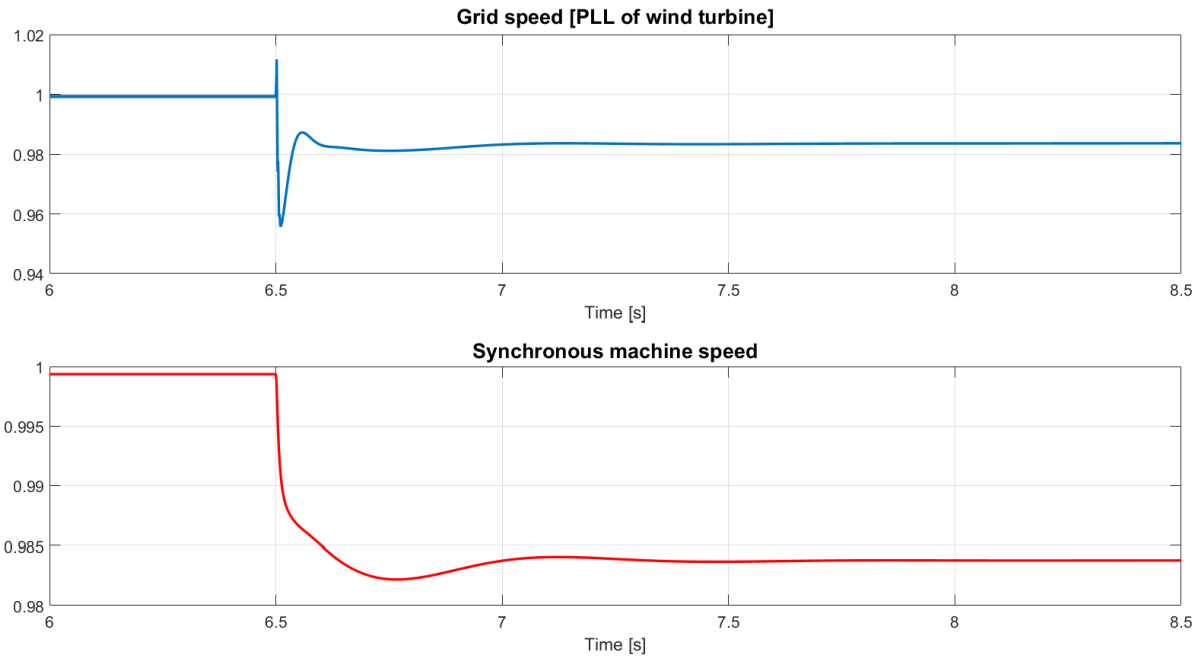


Figure 4.4: Test case 1.1 without VSM: Various system speeds

### 4.1.2 Sudden loss of wind power

Another scenario that demonstrates the dual operation of the SG and the VSM is the case of sudden loss of wind power. In the following case, the wind power suddenly starts to pick up, until it exceeds its limits and stops production. The wind power can be seen in figure 4.6. The wind turbine delivers 0.25 [p.u] of power up until  $t = 6.5[s]$ , when the power starts to pick up. The wind power reach 0.45[p.u] at  $t = 8.5[s]$  and the power is cut.

All parameters remain unchanged from the ones listed in table 4.1. An additional electrical load is not connected, but remains at 0.5 [p.u]. The reference power of the VSM remains at 0, so when the wind power starts to pick up, the power starts to flow into the battery bank; it is charging. This can be seen in 4.5 from  $t = 6.5[s]$  to  $t = 8.5[s]$ . The amount of power that flows into the battery bank and the reduction of power produced by the gas turbine is again determined by the droop constants of the active power controller of the VSM and the governor of the SG.



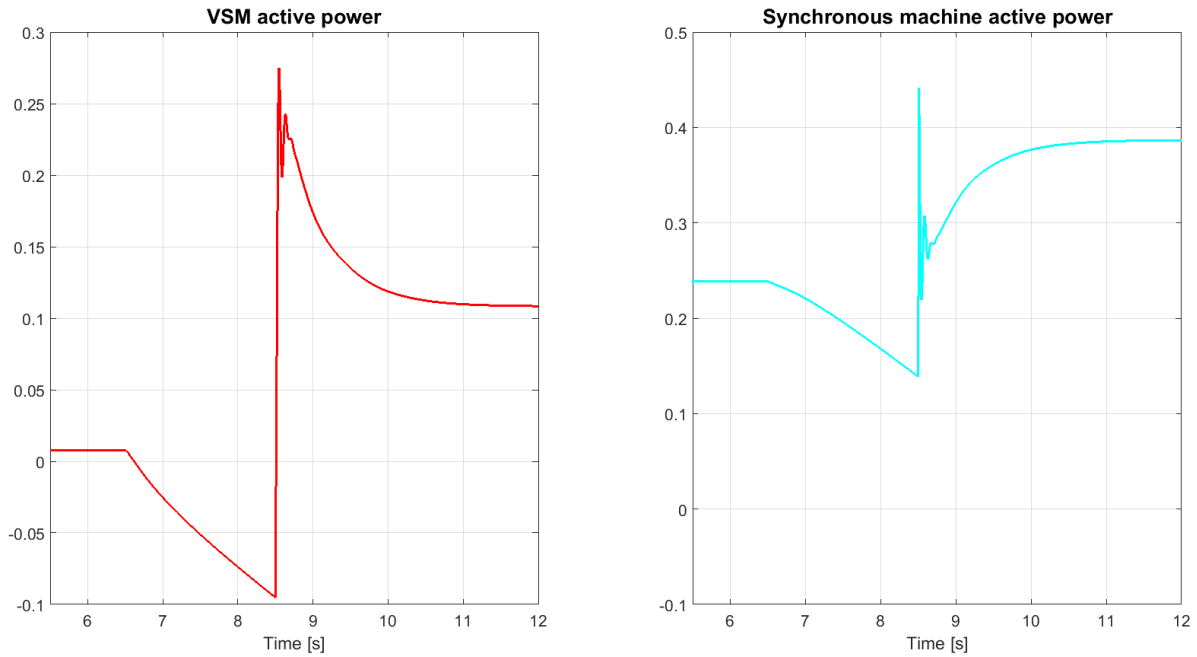


Figure 4.5: Test case 1.2: Active power a)

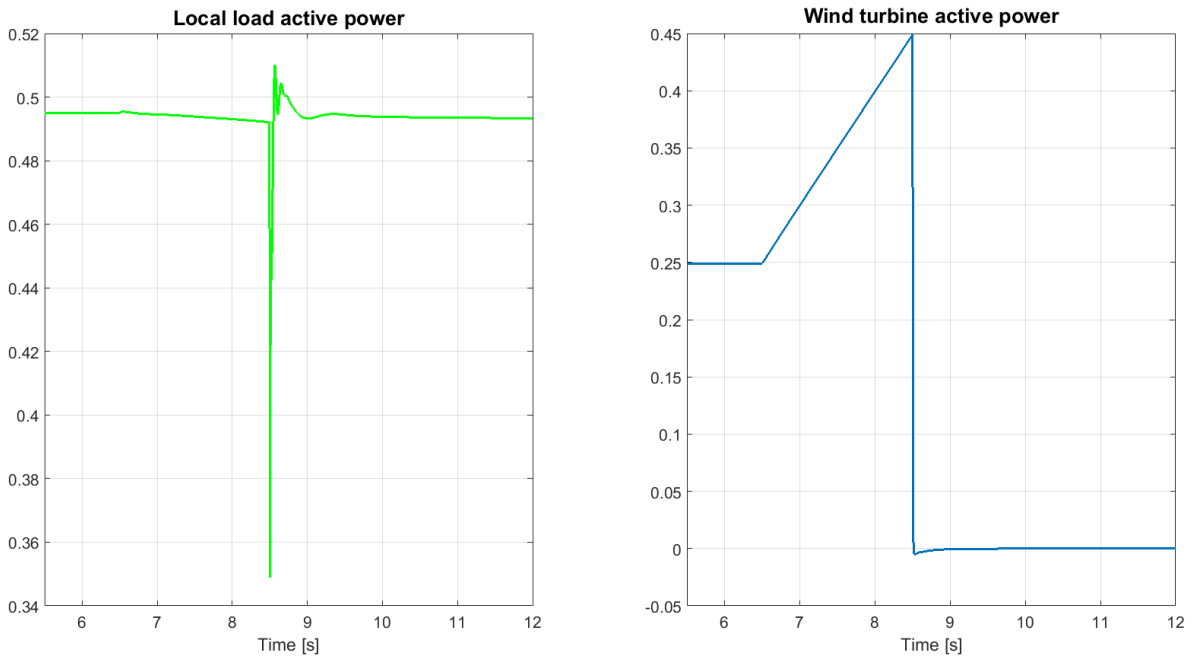


Figure 4.6: Test case 1.2: Active power b)

When the wind power is cut at  $t = 8.5[s]$ , the two sources share the additional load between themselves in the same way they did with the step-up in load in section 4.1.1.

This shows how the VSM can operate in both charging mode and power delivery mode in parallel with a synchronous machine and doing so without altering any settings during the process. There are also a lot of options to tune how the VSM would react in such an event. This can be done by changing the reference power and droop of the VSM and SG.

In figure 4.7 you can see the system speeds. The speed of the system is 1 [p.u] up until  $t = 6.5[s]$  when the wind power is picking up. Then we see an increase in system speed similar to what you would get during a decrease in load. This increase in speed is dictated by the droop of the VSM and governor of the SG. When the wind power is cut at  $t = 8.5[s]$  there is a transient state before the speed stabilizes at a lower level.

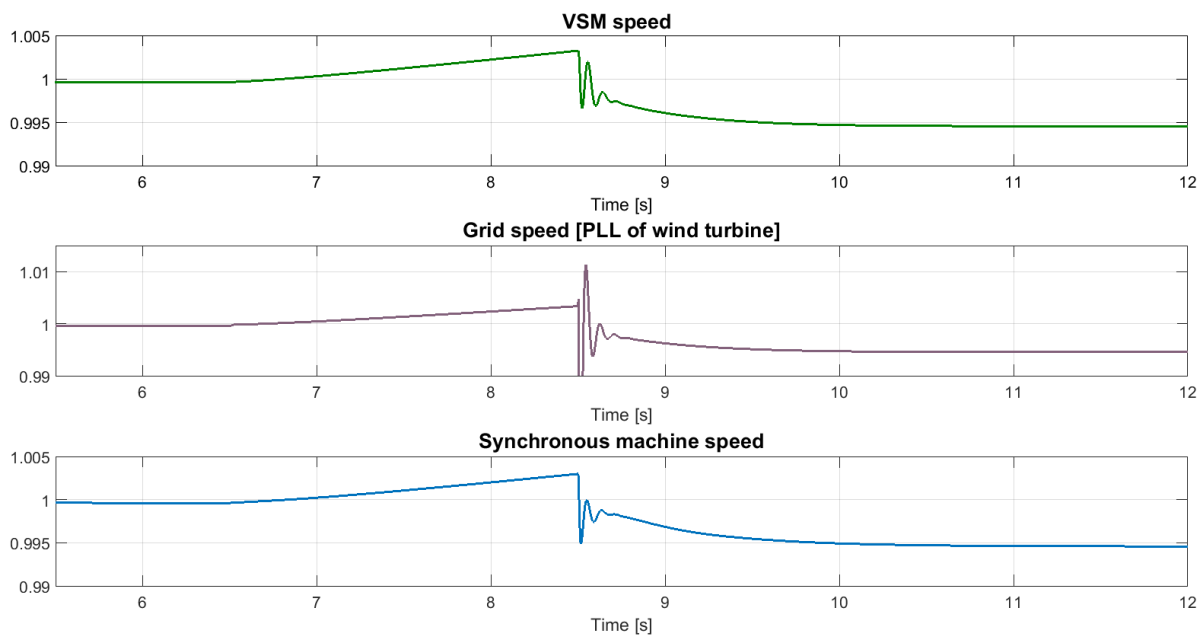


Figure 4.7: Test case 1.2: Various system speeds

## 4.2 Demonstration of Island Operation Capability

This section contains results from scenarios where the goal is to show how the VSM can operate in island operation. The battery bank will in other words be operating without

a SG or a stiff grid and the VSM will have to set the grid frequency and ensure power balance by itself.

### 4.2.1 Operation without gas turbine/SG

This scenario has the SG disconnected from the system and the local load of 0.5 [p.u] is being covered by the wind turbine and the battery bank. The active power reference of the VSM  $p_{VSM}^*$  is 0.5 [p.u] in this scenario.

The wind power from the turbine is initially 0.25 [p.u], but starts to vary at  $t = 6.5[s]$  as shown by the blue line in figure 4.8. The wind power is eventually cut at  $t = 10[s]$  and the battery bank is supplying the local load alone.

As we can see in figure 4.8, the VSM is matching the variations in the wind power and the two graphs seem to be mirrors of each other. The battery bank immediately increases its output when the wind power is lost at  $t = 10[s]$ . Figure 4.9 shows how the speed is varied with the increasing or decreasing loading of the VSM. This illustrates how the speed of the system is determined by the droop controller of the VSM. The speed response at  $t=10[s]$  also show how the inertia of the VSM prevents the speed from dropping too low when the wind power is cut. The rapid increase in power output from the battery bank enables the maintaining of the frequency.

In the beginning of the simulation, at  $t = 5[s]$ , the speed of the system is high; it's over 1.01 [p.u]. This is because the active power reference of the VSM,  $p_{VSM}^*$ , is sat to be 0.5 [p.u], while the reference speed is sat to 1 [p.u]. The speed of the system would be 1 [p.u] if the battery bank were to cover the local load alone, and not with the help of the wind turbine. This shows that a challenge with the islanded VSM system is to tune the references and droop constants in such a way that the frequency is kept within its limits even when there are large variations in the wind power. It might be desirable to use different settings for when you are running parallel to a SG or for various wind conditions.

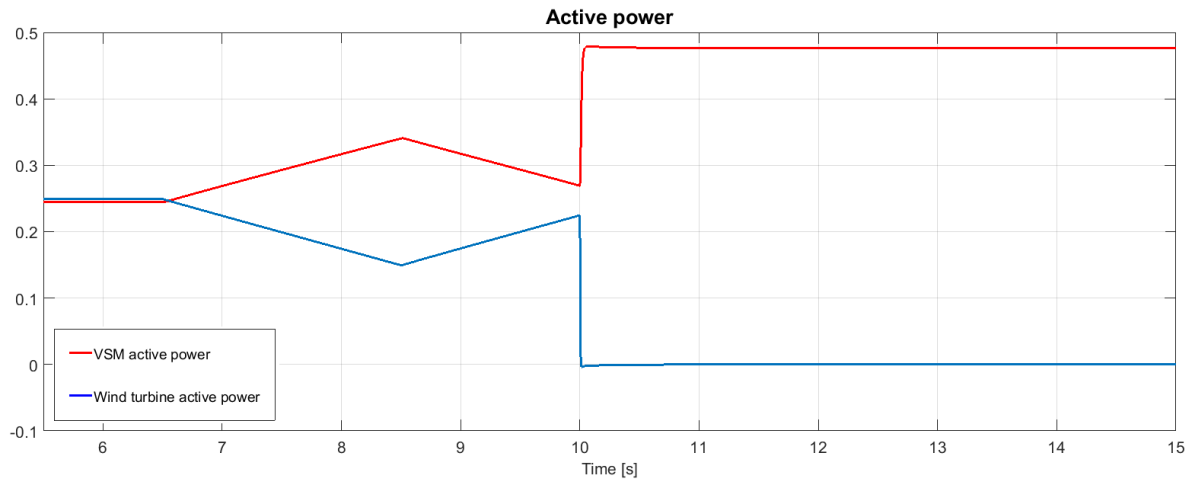


Figure 4.8: Test case 2.1: Active power

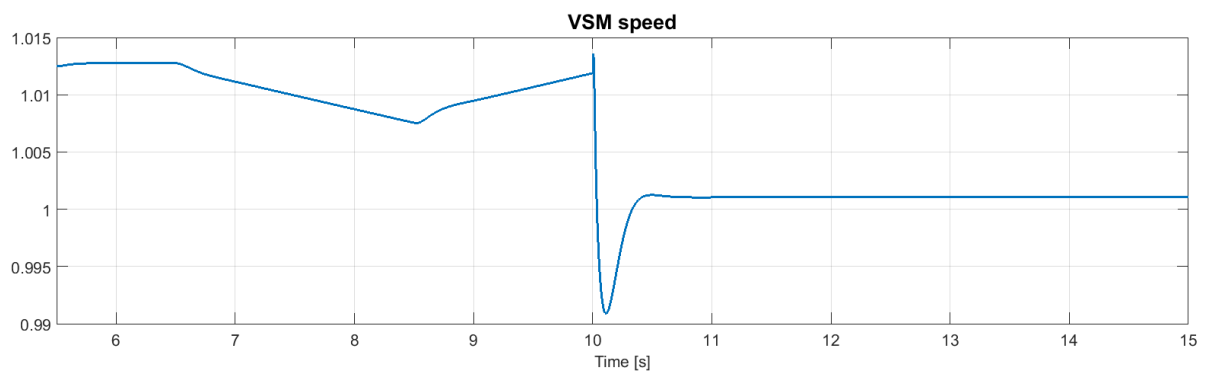


Figure 4.9: Test case 2.1: Speed

### 4.2.2 Step up in reactive power demand

In this scenario there is a sudden increase in reactive power demand from the load. This can represent the starting of a large induction machine; an event that requires a lot of reactive power to set up the rotor field. The increase in reactive load occurs at  $t = 6.5[s]$  and is achieved by adding another impedance the same way as in section 4.1.1. This load however, has double the inductance.

It can be observed in figure 4.10 that the reactive power production from the VSC of the battery bank, named "VSM reactive power" in the figure, increases its production in order to accommodate for the increased demand. The figure also shows a decrease in reactive power from the wind turbine. The reason for this decrease has not been analyzed in detail, but one explanation could be the reduced reactive power production in the filter capacitors connected to the VSC caused by the reduced voltage. The voltage drop can be seen at  $t = 6.5[s]$  in figure 4.11. This reduction in voltage magnitude is caused by the droop-based reactive power controller of the VSM which was described in section 3.2. Equation (3.7) explains how an increased reactive power output,  $q_m$ , will cause a lower voltage reference,  $v^{r*}$ , to be sent to the virtual impedance and the SRF controllers. This will again lower the voltage magnitude at the PCC since the system is in island operation and its voltage is set by the power electronics of the battery bank.

## 4.3 The Effect of the Virtual Inertia of the VSM

This final section will explore the effects of changing the inertia constant  $T_a$  of the VSM. In this scenario, the system experiences a step up in electrical load by connecting an additional impedance in parallel. This increase is the same as the one in section 4.1.1. In this section the SG is disconnected and the wind turbine and battery bank covers the load alone. The wind turbine is producing a constant power of 0.4 [p.u] while the battery bank is covering the remaining load. The load increase occurs at  $t = 6.5[s]$ .

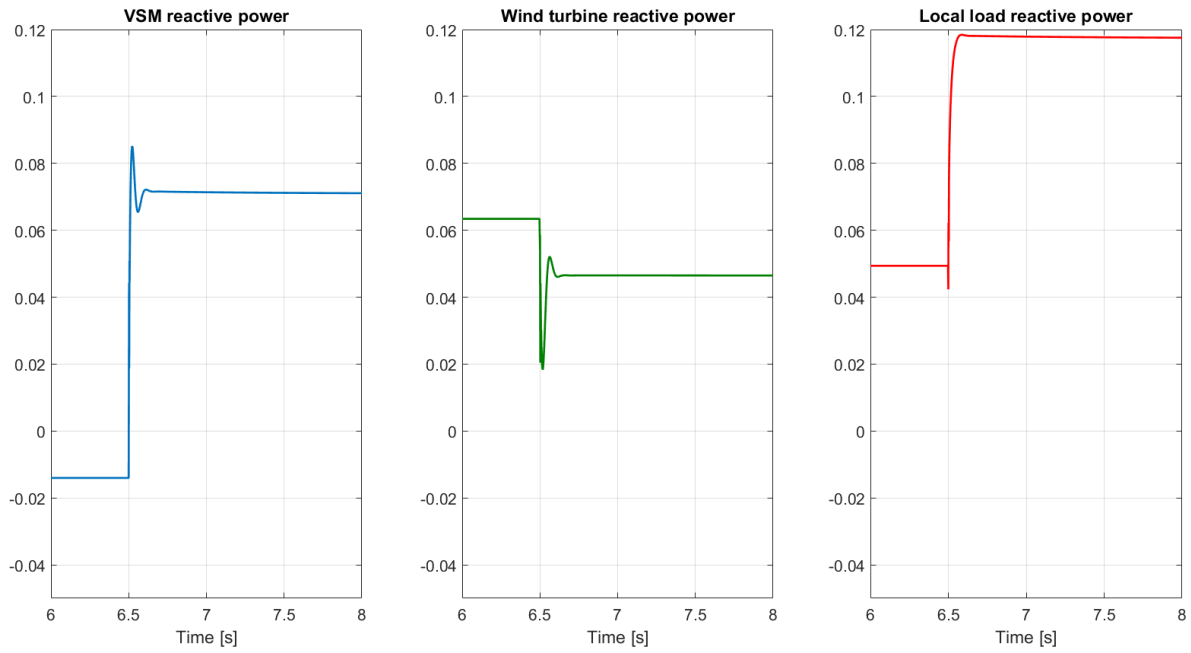


Figure 4.10: Test case 2.2: Reactive power

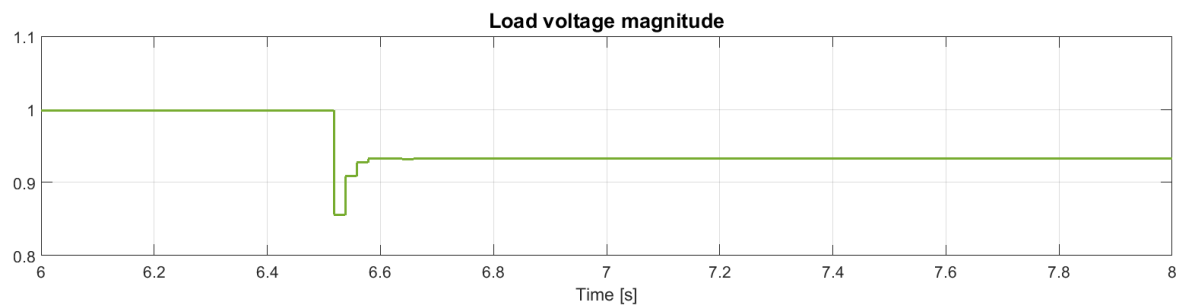


Figure 4.11: Test case 2.2: Load voltage magnitude

The load increase described in the above paragraph has been tested for four different inertia time constants and the different speed responses are presented in figure 4.12. The speed depicted in this figure is the internal speed of the VSM, which is determined by its swing equation, equation(3.5).

It is clear that the immediate drop in speed is larger with a larger inertia, which is what one would expect. The figure also shows how the larger inertia uses longer time to stabilize at its new speed. The new steady state speed is not affected by changing the inertia time constant since it is determined by the droop of the active power controller, as well as the power and speed references.

In this scenario, the immediate drop in speed helps the signal reach its new steady state value faster. This is quite clear for the graphs of  $T_a = 5[s]$  and  $T_a = 10[s]$  since their immediate drops leaves them closer to the new steady state speed than the other two. In addition to this, the lower inertia VSM's also works towards the new steady state speed more rapidly, meaning that they have a steeper curve. The higher inertia, the more energy needs to be added in order to change its speed.

Figure 4.12 also illustrates in a way how the inertia constant of the VSM can be chosen in order to fit the system it is applied to, and in that way obtain a desired speed response. You may also want to run the VSM with different inertias under different states, say in parallel with an SG or when the battery bank is being charged to make sure the responses are acceptable. The choice of the inertia constant can also be combined with the changing of the damping coefficient in order to get the desired behavior. The choice of these parameters can be combined with the choice of speed and power references, as well as droop, to get the desired power and speed responses from the VSM.

The inertia constant also need to be dimensioned according to the current limits of the VSC it is controlling. This is especially important when operating in grid connection or in parallel with large SG's. In those cases, a drop in grid frequency will cause a large increase in power output from the battery bank provided by the damping term of the swing equation. This is less of a pressing matter when operating in island operation where the

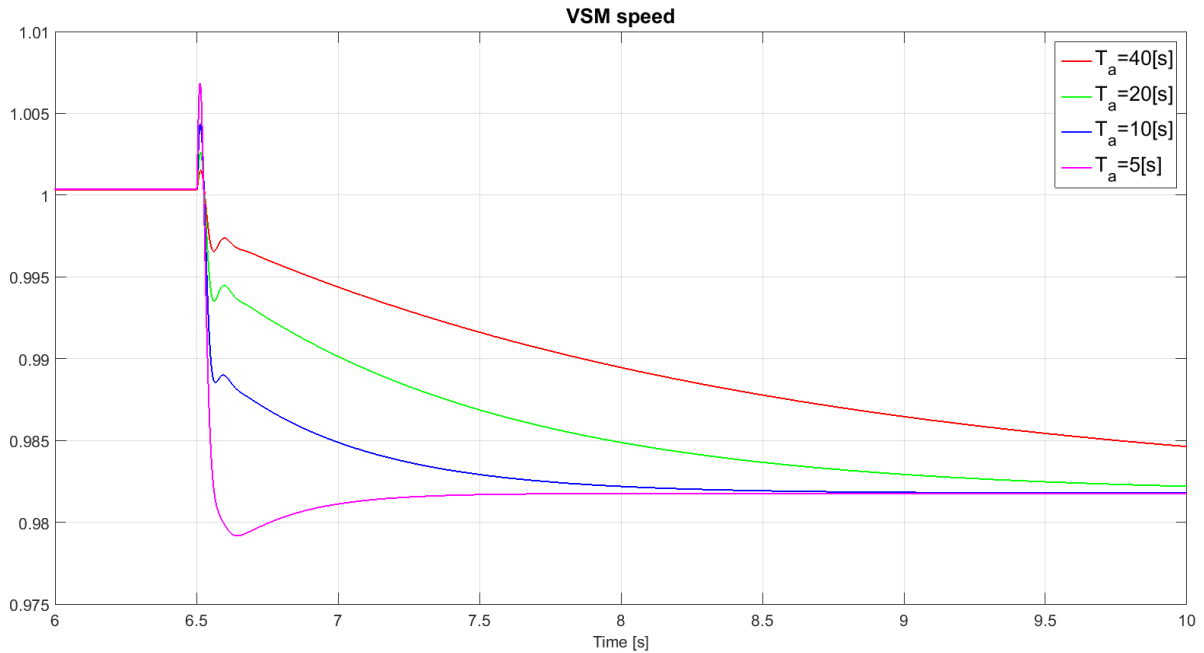


Figure 4.12: Test case 3.1: speed

local load alone is determining the power from the energy sources. A solution could be to use a lower inertia when in grid operation compared to when in island operation if there is a risk of exceeding the current limitations.

The high power output as a result of a decrease in grid speed is demonstrated in figure 4.13. This scenario has the VSM run at a speed of 1.02 [p.u] by changing speed reference  $\omega_{VSM}^*$ . The system is in island operation and with the same wind power and load as before. At  $t = 4[s]$ , the grid is connected and enforce the 1 [p.u] speed on the system. This is causing an immediate increase in power output from the battery bank. This scenario has been simulated with  $T_a = 5[s]$  and  $T_a = 20[s]$ ; you can see in figure 4.13 that the higher inertia constant gives a higher immediate power increase the moment the grid is connected. In the same figure you can see the change in the internal speed of the VSM. The initial drop in speed is, as you would expect, largest for the simulation with the lower inertia.



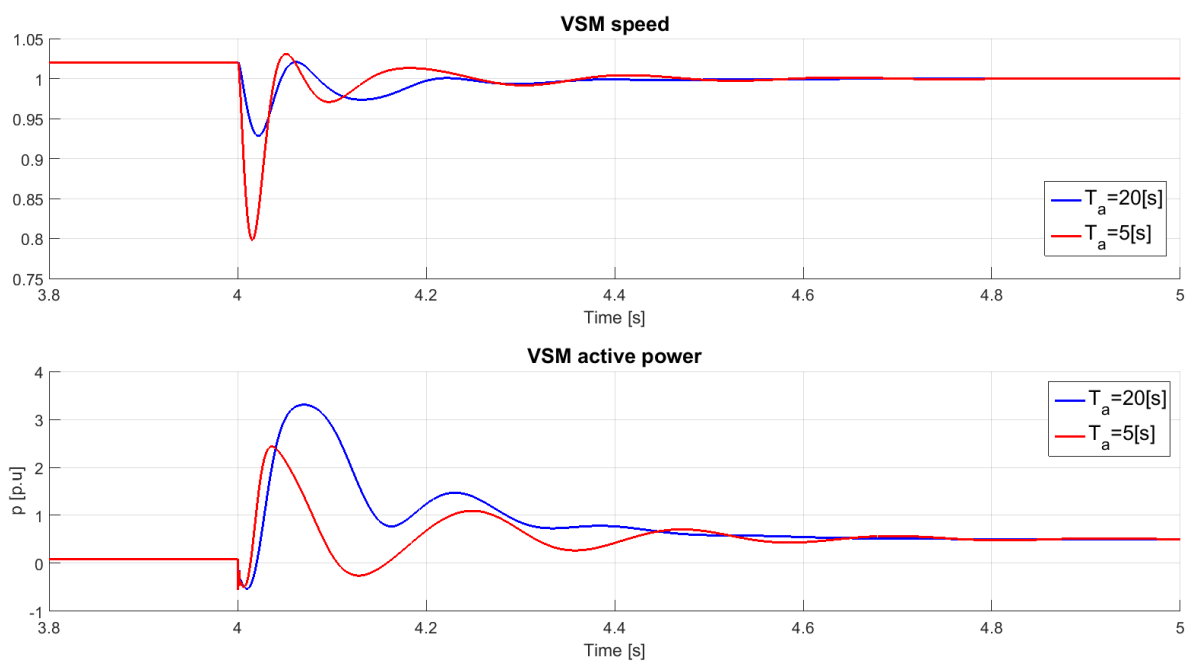


Figure 4.13: Test case 3.2: speed and power



# Chapter 5

## Conclusion

An electrical system was designed for this thesis and its purpose was to represent the grid of an offshore oil and gas platform. The designed system was a considerable simplification of a system that in reality would be a lot more complex. However, the system served its purpose and fitted the scope of this thesis. The low complexity made it easier to study the components that were relevant and to observe how they affected the system.

Said system consists of a synchronous generator powered by a gas turbine, a battery bank operated as a virtual synchronous machine, a wind turbine and a load impedance. All these components were connected to a point of common coupling with a grid impedance in between.

The modeling of the various components has been covered and a model of the system has been implemented into the Matlab®/Simulink® environment with the use of Simscape Power Systems™. Several simplifications were made when modeling the various components. This was done in order to make the simulations easier, and to make the modeling less complex.

This model was explored and experimented with during the work of implementation and the components of the system has been continuously tested with simulations. This was necessary in order to confirm the correct functioning of the various part of the system,

but it also helped to recognize the behavior of the various components.

After completing the implementation of the model began the work of identifying relevant test cases. This work comprised of further exploration of the system in order to recognize scenarios of interest. The effort of identifying test cases also brought about a better understanding of the functionality of the components, as well as the system as a whole.

The first test cases presented in chapter 4 examines the load sharing between the power sources in the system. This was achieved by studying the response in power and speed at the power sources during events such as a sudden load increase or variations in wind power. Further test cases involved the removal of the synchronous generator from the system in order to study the VSM and wind turbine in island operation. This system was subjected to variations in wind power, as well as a predominantly reactive power increase. The latter was carried out in order to examine the functioning of the reactive power controller of the VSM.

These test cases indicates that this VSM implementation has good practical suitability for the interfacing of wind turbines with offshore oil and gas platforms. It performs well in parallel with a traditional synchronous generator, and also has the ability to operate in a power electronic dominated environment where it defines the grid speed with its own swing equation. The VSM also responds to changes in load so it can enable the turning off of gas turbines when enough wind power is present.

The final test cases involved examining in impact of changing the inertia constant of the VSM. Simulations were performed in both grid-connection and island operation in order to address various challenges of setting the inertia constant. It was argued that it might be favorable to use different inertia constants during various modes of operation in order to get a desired response from the VSM.

## 5.1 Recommendations for Further Work

The introduction of this thesis presented several limitations for the work that has been conducted. The main limiting factor is the simplifications of the studied system and the modeling of said system. A more complex system would indeed enable a more detailed analysis and the study of more test cases. A technology to synchronize and connect the VSM to a stiff grid or an operational synchronous generator would for example allow for a whole new range of highly relevant scenarios to be studied.

The model of the system could also be expanded to include more detailed implementations of gas turbines, wind turbines, cables, loads battery banks and converters. This would make it possible to further study the impacts of contingencies on such a system and explore the VSM's response to these events.



# Appendix A

## Figures

### A.0.1 Maturity of wind turbine technology (Source: NVE)[18]

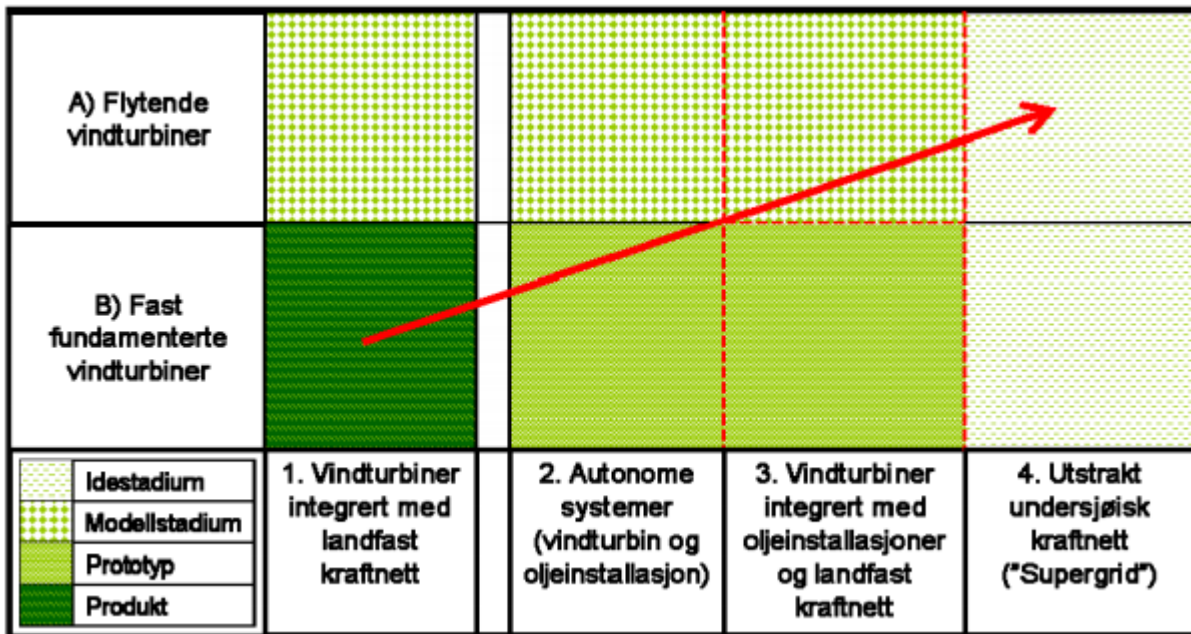


Figure A.1: Maturity of wind turbine technology

# Appendix B

## Screenshots

### B.1 Screenshot from Simulink of SG parameters

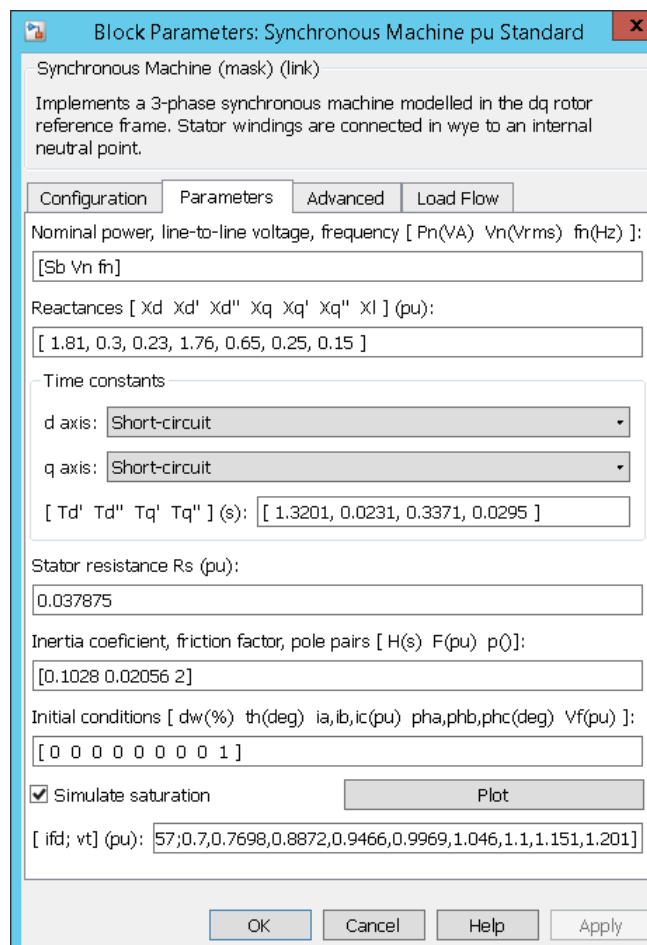


Figure B.1: SG parameters



## B.2 Screenshot from Simulink of system overview

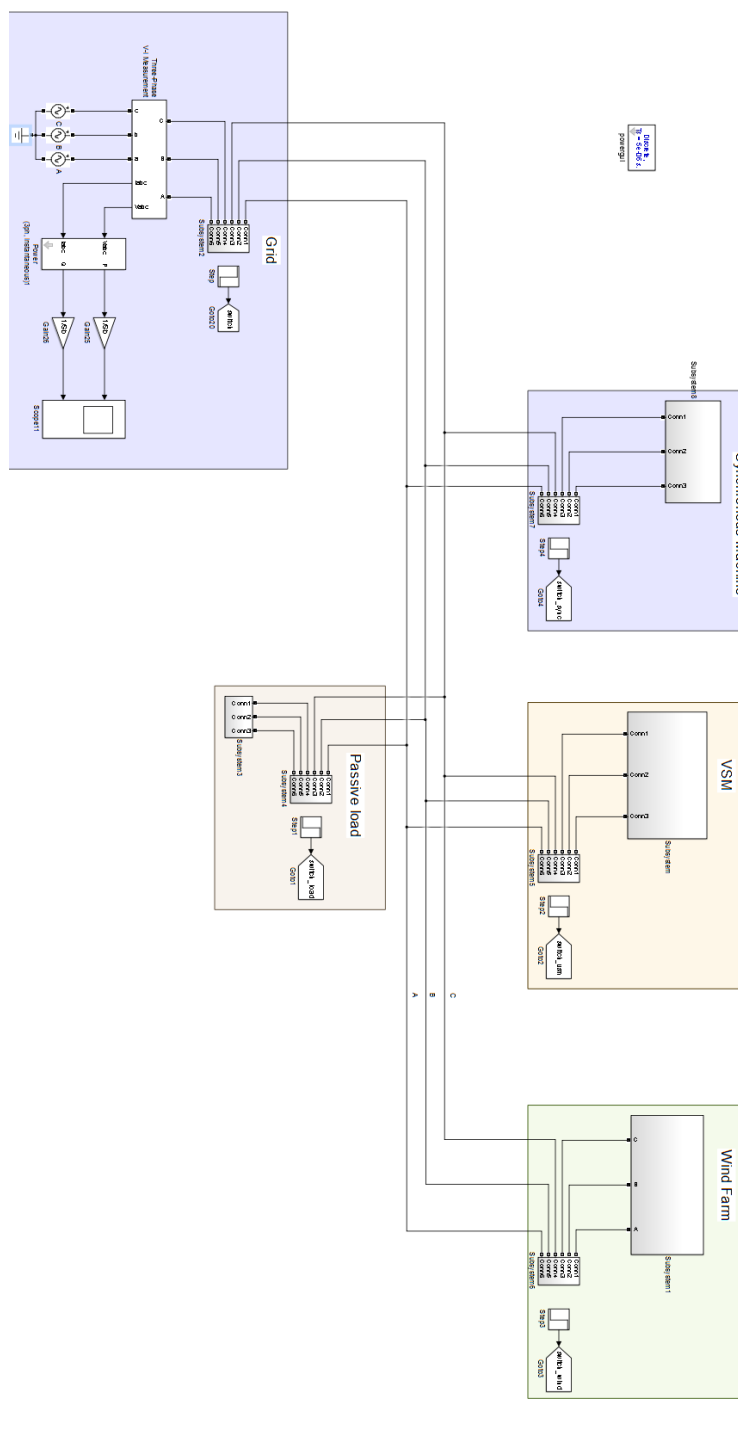


Figure B.2: System overview

### B.3 Screenshot from Simulink of Wind turbine VSC

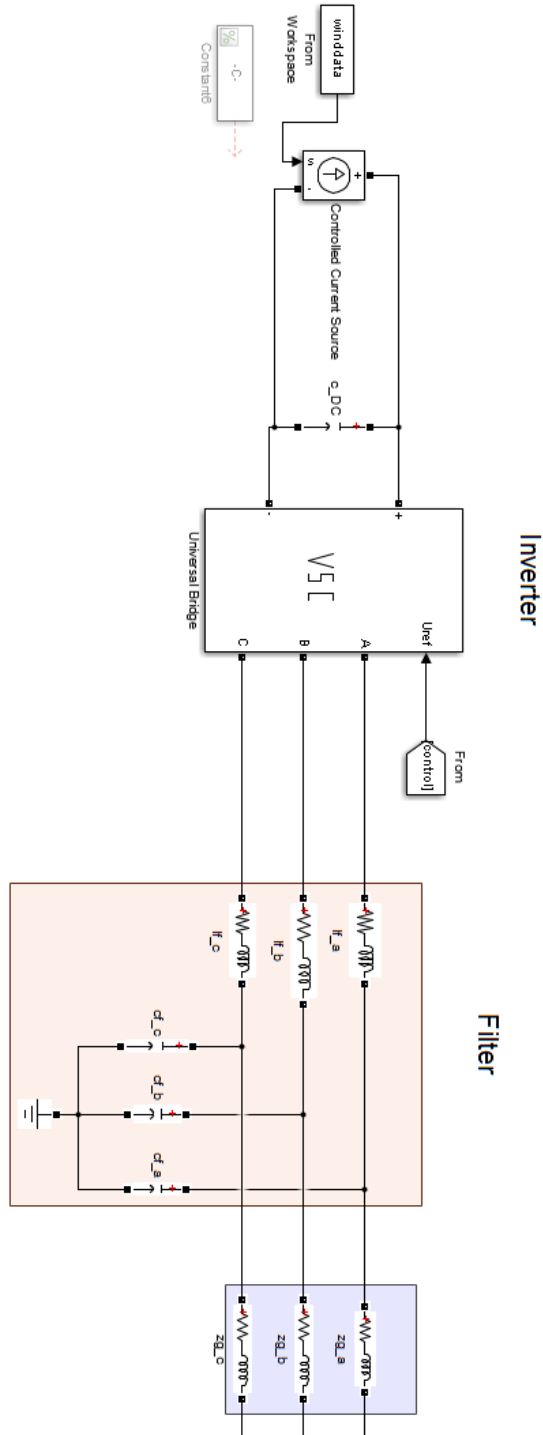


Figure B.3: Wind turbine VSC in Simulink®

## B.4 Screenshot from Simulink of Gas Turbine and SG

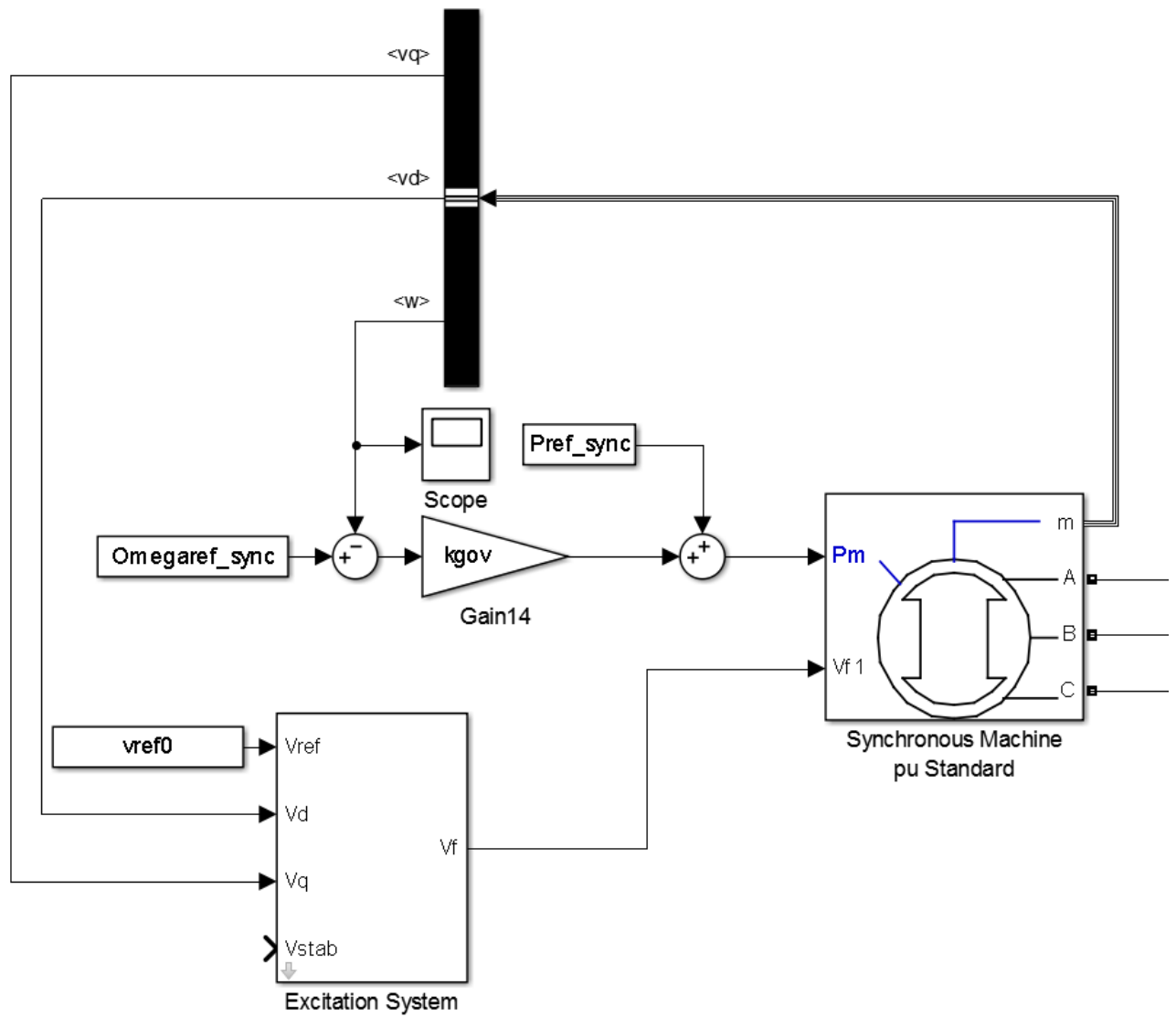


Figure B.4: Gas turbine and SG



# Bibliography

- [1] LORC, <http://www.lorc.dk/offshore-wind-farms-map/sheringham-shoal>, Sheringham Shoal Offshore Wind Farm. Accessed: 19.04.2016.
- [2] Statoil, <http://www.statoil.com/no/TechnologyInnovation/NewEnergy/RenewablePowerProduction/Offshore/HywindScotland/Pages/PilotPark.aspx>, Hywind Scotland Pilot Park. Accessed: 19.04.2016.
- [3] The European Wind Energy Assosiation, <http://www.ewea.org/wind-energy-basics/faq/>, Wind Energy FAQ. Accessed: 02-05-2016.
- [4] The Norwegian Oil and Gas Assosiation, <https://www.norskoljeoggass.no/en/Publica/Environmental-reports/Environmental-report-2015>, Environmental Report 2015. Accessed: 16-11-2015.
- [5] Beck, H.-P. and Hesse, R. (2007). Virtual synchronous machine. *Electrical Power Quality and Utilisation, 2007. EPQU 2007. 9th International Conference*.
- [6] Carrol, J., McDonald, A., and McMillan, D. (2015). Reliability comparison of wind turbines with DFIG and PMG drive trains. *IEEE Transactions on Energy Conversion, Vol. 30, No. 2, June 2015 663*.
- [7] D'Arco, S. and Suul, J. A. (2013). Virtual synchronous machines - classification of implementations and analysis of equivalence to droop controllers for microgrids. *PowerTech (POWERTECH), 2013 IEEE Grenoble*.
- [8] D'Arco, S. and Suul, J. A. (2015). A synchronization controller for grid reconnection of islanded virtual synchronous machines. *2015 IEEE 6th International Symposium on Power Electronics for Distributed Generation Systems (PEDG)IEEE 6th International Symposium on Power Electronics for Distributed Generation Systems (PEDG)*.

- [9] D'Arco, S., Suul, J. A., and Fosso, O. B. (2013). Control system tuning and stability analysis of virtual synchronous machines. *Energy Conversion Congress and Exposition (ECCE), 2013 IEEE*.
- [10] D'Arco, S., Suul, J. A., and Fosso, O. B. (2014). A virtual synchronous machine implementation for distributed control of power converters in smartgrids. *Electric Power Systems Research 122 (2015) 180-197*.
- [11] D'Arco, S., Suul, J. A., and Fosso, O. B. (2015). Small-signal modeling and parametric sensitivity of a virtual synchronous machine in islanded operation. *Electrical Power and Energy Systems 72 (2015) 3-15*.
- [12] Gavenas, E. (2014). On the way to a cleaner future: a study of co2 emissions on the norwegian continental shelf. Master's thesis, Norwegian university of life sciences.
- [13] Haugstad, T. Teknisk Ukeblad, <http://www.tu.no/artikler/snart-kan-oljeselskapene-fa-strom-fra-flytende-havvind-kan-spare-3-dollar-fatet/346957>, Snart kan oljeselskapene få strøm fra flytende havvind - kan spare 3 dollar fatet. Accessed: 04-05-2016.
- [14] Kaura, V. (1997). Operation of a phase locked loop system under distorted utility conditions. *IEEE Trans. Ind. Appl. 33 (January/February (1)) (1997) 58-63*.
- [15] Kolstad, H. (2002). *Control of an Adjustable Speed Hydro utilizing Field Programmable Devices (Ph.D. thesis)*. PhD thesis, Norwegian University of Science and Technology.
- [16] Machowski, J., Bialek, J. W., and Bumby, J. R. (2008). *Power System Dynamics: Stability and Control. - 2nd ed.* John Wiley & Sons, Ltd.
- [17] Mathisen, E. R. (2015). Application and analysis of virtual synchronous machines in marine and offshore grids. Specializing project at NTNU.
- [18] NVE, Oljedirektoratet, Petroleumstilsynet, and Statens Forurensningstilsyn (2008). Kraft fra land til norsk sokkel.

- [19] Ramsdal, R. Teknisk ukeblad, <http://www.tu.no/artikler/disse-5-feltene-slipper-ut-mest-pa-sokkelen/230485>, Disse 5 feltene slipper ut mest på sokkelen. Accessed: 26-04-2016.
- [20] Toftevaag, T. (2015a). Course TET 4200 marine and offshore power systems: Parallel operation of ac generators. NTNU.
- [21] Toftevaag, T. (2015b). Course TET 4200 marine and offshore power systems: Turbines and turbine governors. NTNU.